

Multiple Regression for Matrix and Vector Predictors: Models, Theory, Algorithms, and Beyond

Meixia Lin*

Ziyang Zeng†

Yangjing Zhang‡

January 14, 2025

Abstract

Matrix regression plays an important role in modern data analysis due to its ability to handle complex relationships involving both matrix and vector variables. We propose a class of regularized regression models capable of predicting both matrix and vector variables, accommodating various regularization techniques tailored to the inherent structures of the data. We establish the consistency of our estimator when penalizing the nuclear norm of the matrix variable and the ℓ_1 norm of the vector variable. To tackle the general regularized regression model, we propose a unified framework based on an efficient preconditioned proximal point algorithm. Numerical experiments demonstrate the superior estimation and prediction accuracy of our proposed estimator, as well as the efficiency of our algorithm compared to the state-of-the-art solvers.

1 Introduction

In the modern big data era, it is commonplace to encounter data sets comprising both matrix and vector variate observations in various fields such as neuroimaging, transportation, and longitudinal studies, where data often exhibits multi-dimensional structures. For example, the recent COVID-19 pandemic, which has led to significant global morbidity and mortality, underscores the importance of developing predictive tools for managing infectious diseases. The COVID-19 Open Data [52] offers a rich repository of daily time-series data on COVID-19 cases, deaths, recoveries, testing, vaccinations, as well as hospitalizations, spanning over 230 countries, 760 regions, and 12,000 lower-level administrative divisions. This data set provides a unique opportunity to develop predictive models that can forecast the spread of the virus. By considering the total number of confirmed cases in each region over a specific period as the response variable, researchers can naturally employ the time-series data to construct a matrix predictor. Simultaneously, other variables with minimal variation during the target period, such as certain health-related characteristics, can serve as vector-valued predictors. In addition to the COVID-19 data, other examples involving both matrix and vector variables include the bike sharing data [13], and the electroencephalography (EEG) data applied in diverse areas like predicting alcoholism [2] and the emotion recognition [40]. To handle such data structures, Zhou and Li [60] proposed a matrix regression model

$$y_i = \langle X_i, B \rangle + \langle z_i, \gamma \rangle + \varepsilon_i, \quad i = 1, \dots, n, \quad (1)$$

where $\{(y_i, X_i, z_i), i = 1, \dots, n\}$ are the observed data. Here $y_i \in \mathbb{R}$ is the response, $X_i \in \mathbb{R}^{m \times q}$ is the matrix variate, $z_i \in \mathbb{R}^p$ is the vector variate, $B \in \mathbb{R}^{m \times q}$, $\gamma \in \mathbb{R}^p$ are the unknown

*Engineering Systems and Design, Singapore University of Technology and Design, Singapore. Email: meixia.lin@sutd.edu.sg

†Department of Mathematics, National University of Singapore, Singapore. Email: ziyangzeng@u.nus.edu

‡Institute of Applied Mathematics, Academy of Mathematics and Systems Science, Chinese Academy of Sciences, Beijing, China. Email: yangjing.zhang@amss.ac.cn

regression coefficients, and ε_i 's are independent and identically distributed random noise, each following a normal distribution with mean 0 and standard deviation σ .

Given the formulation of model (1) and the high dimensionality encountered in various applications, it is often presumed that the coefficients of the models exhibit some special structures such as sparsity and low-rankness. For instance, data sets like the COVID-19 Open Data, typically contain multiple features with longitudinal variability and the features that are relatively constant. See also [11, 12, 19], which assume a rank-1 canonical polyadic decomposition structure for the matrix variate. To address this challenge, we propose a class of regularized regression models capable of predicting structured matrix and vector variables. Given samples $\{(y_i, X_i, z_i), i = 1, \dots, n\}$, we estimate the unknown regression coefficients B and γ through solving the following regularized optimization problem

$$\min_{B \in \mathbb{R}^{m \times q}, \gamma \in \mathbb{R}^p} \sum_{i=1}^n \ell(\langle X_i, B \rangle + \langle z_i, \gamma \rangle, y_i) + \phi(B) + \psi(\gamma), \quad (2)$$

where $\ell : \mathbb{R} \times \mathbb{R} \rightarrow \mathbb{R}$ is a loss function, commonly chosen as the squared loss function $\ell(s_i, y_i) = (y_i - s_i)^2$. Here $\phi : \mathbb{R}^{m \times q} \rightarrow (-\infty, \infty]$ and $\psi : \mathbb{R}^p \rightarrow (-\infty, \infty]$ are given closed proper convex functions, which serve as the penalty functions (also known as regularizers) encouraging special structures in B and γ . Regularization is important due to the potential high dimensionality and intricate structure of the matrix and vector predictors. Commonly used penalty functions of vectors include the lasso [49], the fused lasso [50], the (sparse) group lasso [57, 14], and many others. For the matrix variate, the true predictor often exhibits a low-rank structure or can be well approximated by one. As such, a typical choice of the penalty function is the nuclear norm [36, 51]. There are also other penalty functions of matrices such as multivariate (sparse) group lasso [39, 32] and matrix-type fused lasso [26].

In the literature, various regularized regression models based on (1) have also been studied. Initially, Zhou and Li [60] considered model (3) with $\psi(\cdot) = 0$ and $\phi(\cdot)$ being spectral regularization, such as $\phi(B) = \|B\|_*$. In other words, their focus was primarily on estimating the matrix covariate without applying penalties to the vector part. Similarly, Elsener and van de Geer [8] considered model (3) with matrix variate only by assuming $\gamma = 0$, and they used the absolute value loss and the Huber loss, together with a nuclear norm penalty $\phi(B) = \|B\|_*$. Later, Li and Kong [26] introduced matrix regression with a double fused lasso penalized least absolute deviation (LAD). That is, $\ell(s_i, y_i) = |y_i - s_i|$, with matrix-type fused lasso penalty $\phi(B) = \lambda_1 \|B\|_* + \lambda_2 \sum_{j=2}^m \|B_{j\cdot} - B_{(j-1)\cdot}\|_1$ and vector-type fused lasso penalty $\psi(\gamma) = \lambda_3 \|\gamma\|_1 + \lambda_4 \sum_{j=2}^p |\gamma_j - \gamma_{j-1}|$. Subsequently, Li et al. [27, 28] proposed double fused lasso regularized linear and logistic regression. All these models serve as specific cases of (2). In addition, our model (3) accommodates both vector and matrix coefficients simultaneously and simplifies to the regularized matrix-variate (or vector-variate) regression model [6, 8, 10, 49, 50] under appropriate settings, illustrating its versatility and adaptability to both simpler and more complex scenarios involving various loss and penalty functions. As an increasing number of problems align with this framework, it becomes imperative to develop efficient algorithms to solve it.

Let $\text{vec}(\cdot)$ be the operator stacking the columns of a matrix on top of one another into a vector. Denote $y = (y_1, \dots, y_n)^\top \in \mathbb{R}^n$, $Z = (z_1, \dots, z_n)^\top \in \mathbb{R}^{n \times p}$, and $X = (\text{vec}(X_1), \dots, \text{vec}(X_n))^\top \in \mathbb{R}^{n \times mq}$. Problem (2) can be written in a compact and general form:

$$\min_{B \in \mathbb{R}^{m \times q}, \gamma \in \mathbb{R}^p} \left\{ G(B, \gamma) := \hat{\ell}(X \text{vec}(B) + Z\gamma, y) + \phi(B) + \psi(\gamma) \right\}, \quad (3)$$

where $\hat{\ell} : \mathbb{R}^n \times \mathbb{R}^n \rightarrow \mathbb{R}$ is a loss function. In particular, problem (3) reduces to (2) if we take $\hat{\ell}(s, y) = \sum_{i=1}^n \ell(s_i, y_i)$, for $s, y \in \mathbb{R}^n$. More generally, problem (3) can also incorporate the square root loss function $\hat{\ell}(s, y) = \sqrt{\sum_{i=1}^n (y_i - s_i)^2 / n}$, which is not covered in the form of

problem (2). Throughout the paper, we make the blanket assumption that $\hat{\ell}(\cdot, y)$ is a convex function for any $y \in \mathbb{R}^n$.

In current research, the state-of-the-art first-order methods, including those based on Nesterov algorithm and the alternating direction method of multipliers (ADMM), are prevalent in previously discussed matrix regression models, with various adaptations for different regularization strategies. Specifically, Zhou and Li [60] implemented the Nesterov algorithm for matrix regression problems, focusing on the nuclear norm regularizer. Later, Li and Kong [26] introduced a symmetric Gauss-Seidel based ADMM (sGS-ADMM) to tackle matrix regression problems with a double fused lasso penalized LAD. Subsequently, Li et al. [28] extended this approach to address double fused lasso regularized linear and logistic regression problems. Additionally, a linearized ADMM [27] was proposed for matrix regression problems incorporating both fused lasso and nuclear norm penalties. Fan et al. [9, 10] also implemented a contractive Peaceman-Rachford splitting method to solve their matrix optimization problem. Despite their effectiveness, these first-order methods suffer from slow convergence, especially in the context of the large-scale data. Additionally, they often only leverage first-order information in the underlying non-smooth optimization model. In contrast, in recent study on vector-variate regression with lasso-type penalties [29, 30, 58, 35, 33, 34] and matrix-variate problem with nuclear or spectral norm penalties [21, 22, 5], researchers have designed the semismooth Newton (SSN) based algorithms, which fully take advantage of the second-order information of the problem, to solve the optimization problem efficiently. These appealing evidences suggest the potential for designing a significantly more efficient algorithm that wisely exploits the inherent second-order structured sparsity of vector and special structure of matrix in the matrix regression problems. However, no research has yet leveraged this valuable insight to address problems involving both matrix and vector variables simultaneously. Thus, we aim to design a highly efficient second-order type, dual Newton method based proximal point algorithm (PPDNA) for solving the dual problem of the matrix regression problem (3) with both matrix and vector variables.

In this paper, we propose a class of regularized regression models in the form of (3) to estimate the matrix and vector predictors simultaneously. Our contributions are threefold. First, our model accommodates a range of general convex penalty functions for ϕ and ψ , including the nuclear norm for ϕ , as well as the lasso, the fused lasso, and the group lasso for ψ . Second, we establish the n -consistency and \sqrt{n} -consistency of the estimator from (3) with ϕ defined by the nuclear norm and ψ defined by the ℓ_1 norm. Third, we propose an efficient preconditioned proximal point algorithm for solving the general problem (3).

The rest of the paper is organized as follows. We establish the estimator consistency in Section 2 and develop a preconditioned proximal point algorithm for solving the regularized regression problem (3) in Section 3. Extensive numerical experiments are presented in Section 4. Finally, we conclude the paper in Section 5.

Notations and preliminaries. The linear map $\text{vec} : \mathbb{R}^{m \times q} \rightarrow \mathbb{R}^{mq}$ is defined as follows: for a matrix $Y \in \mathbb{R}^{m \times q}$, $\text{vec}(Y) \in \mathbb{R}^{mq}$ is the column vector obtained by stacking the columns of Y on top of one another. The linear map $\text{mat} : \mathbb{R}^{mq} \rightarrow \mathbb{R}^{m \times q}$ is the adjoint operator of vec , which is defined as follows: for a vector $y \in \mathbb{R}^{mq}$, $\text{mat}(y) \in \mathbb{R}^{m \times q}$ is the matrix obtained by reshaping the elements of y back into a matrix with m rows and q columns, preserving the order of the elements. For $x \in \mathbb{R}$, $x_+ := \max\{x, 0\}$, and $\text{sgn}(x)$ denotes the sign function of x , that is $\text{sgn}(x) = 1$ if $x > 0$; $\text{sgn}(x) = 0$ if $x = 0$; $\text{sgn}(x) = -1$ if $x < 0$. Let $h : \mathbb{R}^n \rightarrow (-\infty, \infty]$ be a closed proper convex function. The Moreau envelope of h at x is defined by

$$E_h(x) := \min_{y \in \mathbb{R}^n} h(y) + \frac{1}{2} \|y - x\|^2, \quad (4)$$

and the corresponding proximal mapping $\text{Prox}_h(x)$ is defined as the unique optimal solution of (4). It follows from Moreau [38] and Yosida [56] that for any $x \in \mathbb{R}^n$, $\nabla E_h(x) = x - \text{Prox}_h(x)$, and $\text{Prox}_h(\cdot)$ is Lipschitz continuous with modulus 1. For $x \in \mathbb{R}^p$, let $\|x\|_1$ and $\|x\|$ be its

ℓ_1 norm and ℓ_2 norm, respectively. For a matrix $X \in \mathbb{R}^{m \times q}$, we use $\|X\|_2$, $\|X\|_F$, $\|X\|_*$, and $\|X\|_\infty$ to denote the spectral norm, Frobenius norm, nuclear norm, and ℓ_∞ norm, respectively. For $f: \mathbb{R}^m \rightarrow \mathbb{R}^n$, $g: \mathbb{R}^p \rightarrow \mathbb{R}^m$, we denote their composition as $(f \circ g)(x) = f(g(x))$, $x \in \mathbb{R}^p$. Define $[n] := \{1, \dots, n\}$. We denote \odot as the Hadamard product, which is an element-wise multiplication of two matrices of the same size. Let \mathbb{S}^n be the space of $n \times n$ symmetric matrices and \mathbb{S}_+^n be the cone of symmetric positive semidefinite matrices. We use $X \succeq Y$ to denote $X - Y \in \mathbb{S}_+^n$. For a locally Lipschitz continuous function $\mathcal{F}: \mathbb{R}^n \rightarrow \mathbb{R}^m$, the Bouligand subdifferential (B-subdifferential) of \mathcal{F} is denoted as $\partial_B \mathcal{F}$, and the Clarke generalized Jacobian of \mathcal{F} is denoted as $\partial \mathcal{F}$.

2 Consistency Analysis

In this section, we analyze the consistency and limiting distributions of our proposed estimator, through studying the asymptotic behavior of the objective function. As a representative example, we consider the following matrix regression problem:

$$\min_{U \in \mathbb{R}^{m \times q}, \beta \in \mathbb{R}^p} \left\{ Z_n(U, \beta) := \frac{1}{n} \sum_{i=1}^n (y_i - \langle X_i, U \rangle - \langle z_i, \beta \rangle)^2 + \frac{\rho_n}{n} \|U\|_* + \frac{\lambda_n}{n} \|\beta\|_1 \right\}. \quad (5)$$

It is a special case of (3) where the loss function $\hat{\ell}$ takes the mean squared error, the penalty function ϕ is proportional to the nuclear norm of the matrix variate, and the penalty function ψ is proportional to the ℓ_1 norm of the vector variate. For given n , ρ_n , and λ_n , we denote $(\hat{B}_n, \hat{\gamma}_n)$ as a solution of (5). We aim to analyze the consistency and limiting distribution of $(\hat{B}_n, \hat{\gamma}_n)$. We first give the following regularity assumptions. It is worth noting that this assumption is similar to those commonly used in the literature to establish consistency for various estimators, including the least absolute deviation estimator [1, 42], Lasso-type penalized regression models [23], and regularized matrix regression estimators [28, 54].

Assumption 1. We assume that the following regularity conditions hold:

$$C_n := \frac{1}{n} \sum_{i=1}^n \text{vec}(X_i) \text{vec}(X_i)^\top \rightarrow C, \quad D_n := \frac{1}{n} \sum_{i=1}^n z_i z_i^\top \rightarrow D, \quad H_n := \frac{1}{n} \sum_{i=1}^n \text{vec}(X_i) z_i^\top \rightarrow H,$$

where $C \in \mathbb{S}_+^{mq}$, $D \in \mathbb{S}_+^p$, and $H \in \mathbb{R}^{mq \times p}$.

Under the above assumption, we further denote

$$S_n := \begin{pmatrix} C_n & H_n \\ H_n^\top & D_n \end{pmatrix} \rightarrow S := \begin{pmatrix} C & H \\ H^\top & D \end{pmatrix}. \quad (6)$$

It can be seen that S_n and S are positive semidefinite, since for any $u \in \mathbb{R}^{mq}$ and $v \in \mathbb{R}^p$, it holds that

$$\begin{aligned} (u^\top \quad v^\top) S_n \begin{pmatrix} u \\ v \end{pmatrix} &= \frac{1}{n} \sum_{i=1}^n (u^\top \text{vec}(X_i) \text{vec}(X_i)^\top u + 2u^\top \text{vec}(X_i) z_i^\top v + v^\top z_i z_i^\top v) \\ &= \frac{1}{n} \sum_{i=1}^n (u^\top \text{vec}(X_i) + v^\top z_i)^2 \geq 0. \end{aligned}$$

Note that when the matrix S_n is positive definite, the estimator $(\hat{B}_n, \hat{\gamma}_n)$ is unique.

The following theorem shows the n -consistency of the estimator $(\hat{B}_n, \hat{\gamma}_n)$. For penalty parameters $\rho_n = o(n)$ and $\lambda_n = o(n)$, the estimator $(\hat{B}_n, \hat{\gamma}_n)$ converges to the true regression coefficients (B, γ) in probability as $n \rightarrow \infty$. We outline the proof of Theorem 2.1 here, with a detailed proof in Appendix A.

Theorem 2.1. Suppose Assumption 1 holds and S in (6) is positive definite. If $\rho_n/n \rightarrow \rho_0 \geq 0$ and $\lambda_n/n \rightarrow \lambda_0 \geq 0$, then

$$(\hat{B}_n, \hat{\gamma}_n) \rightarrow (\hat{B}, \hat{\gamma}) := \arg \min_{U \in \mathbb{R}^{m \times q}, \beta \in \mathbb{R}^p} Z(U, \beta)$$

in probability as $n \rightarrow \infty$, where

$$Z(U, \beta) := \begin{pmatrix} \text{vec}(U - B) \\ \beta - \gamma \end{pmatrix}^\top S \begin{pmatrix} \text{vec}(U - B) \\ \beta - \gamma \end{pmatrix} + \rho_0 \|U\|_* + \lambda_0 \|\beta\|_1.$$

In particular, if $\rho_n = o(n)$ and $\lambda_n = o(n)$, then $\arg \min_{U \in \mathbb{R}^{m \times q}, \beta \in \mathbb{R}^p} Z(U, \beta) = (B, \gamma)$ and therefore $(\hat{B}_n, \hat{\gamma}_n)$ is consistent.

Sketch of proof. First, we show that $Z_n(U, \beta) - Z(U, \beta) \rightarrow \sigma^2$ in probability as $n \rightarrow \infty$. By the definitions of Z_n and Z , we have

$$\begin{aligned} Z_n(U, \beta) - Z(U, \beta) &= \text{vec}(U - B)^\top (C_n - C) \text{vec}(U - B) + (\beta - \gamma)^\top (D_n - D) (\beta - \gamma) \\ &\quad + 2 \text{vec}(U - B)^\top (H_n - H) (\beta - \gamma) + \left(\frac{\rho_n}{n} - \rho_0 \right) \|U\|_* \\ &\quad + \left(\frac{\lambda_n}{n} - \lambda_0 \right) \|\beta\|_1 + \frac{1}{n} \sum_{i=1}^n \varepsilon_i^2 - \frac{2}{n} \sum_{i=1}^n \varepsilon_i (\langle X_i, U - B \rangle + \langle z_i, \beta - \gamma \rangle). \end{aligned}$$

Then we show that $\frac{1}{n} \sum_{i=1}^n \varepsilon_i (\langle X_i, U - B \rangle + \langle z_i, \beta - \gamma \rangle) \rightarrow 0$ in probability and therefore the first step completes. By Pollard [42], it further holds that, for any compact set $K \subset \mathbb{R}^{m \times q} \times \mathbb{R}^p$,

$$\sup_{(U, \beta) \in K} \left| Z_n(U, \beta) - Z(U, \beta) - \sigma^2 \right| \rightarrow 0 \text{ in probability as } n \rightarrow \infty. \quad (7)$$

Second, we show the sequence $\{(\hat{B}_n, \hat{\gamma}_n)\}$ is bounded in probability via showing the boundedness of $\{(\hat{B}_n^{(0)}, \hat{\gamma}_n^{(0)})\}$, defined by

$$(\hat{B}_n^{(0)}, \hat{\gamma}_n^{(0)}) := \arg \min_{U \in \mathbb{R}^{m \times q}, \beta \in \mathbb{R}^p} \left\{ Z_n^{(0)}(U, \beta) := \frac{1}{n} \sum_{i=1}^n (y_i - \langle X_i, U \rangle - \langle z_i, \beta \rangle)^2 \right\}.$$

The boundedness of $\{(\hat{B}_n, \hat{\gamma}_n)\}$ then ensures the applicability of (7).

Finally, we establish the convergence $(\hat{B}_n, \hat{\gamma}_n) \rightarrow (\hat{B}, \hat{\gamma})$ in probability by showing the convergence $Z(\hat{B}_n, \hat{\gamma}_n) \rightarrow Z(\hat{B}, \hat{\gamma})$, leveraging the fact that $Z(\cdot, \cdot)$ is strongly convex. ■

As stated in the above theorem, n -consistency of the estimator $(\hat{B}_n, \hat{\gamma}_n)$ requires $\rho_n = o(n)$ and $\lambda_n = o(n)$. However, for \sqrt{n} -consistency of $(\hat{B}_n, \hat{\gamma}_n)$, we require penalty parameters grow more slowly: $\rho_n = o(\sqrt{n})$, $\lambda_n = o(\sqrt{n})$, as shown in the following theorem.

Theorem 2.2. Suppose Assumption 1 holds and S in (6) is positive definite. If $\rho_n/\sqrt{n} \rightarrow \rho_0 \geq 0$ and $\lambda_n/\sqrt{n} \rightarrow \lambda_0 \geq 0$, then

$$\sqrt{n}(\hat{B}_n - B, \hat{\gamma}_n - \gamma) \rightarrow \arg \min_{U \in \mathbb{R}^{m \times q}, \beta \in \mathbb{R}^p} F(U, \beta)$$

in distribution as $n \rightarrow \infty$, where

$$\begin{aligned} F(U, \beta) &:= \text{vec}(U)^\top C \text{vec}(U) + \beta^\top D \beta + 2 \text{vec}(U)^\top H \beta - 2 \text{vec}(U)^\top w_1 - 2 \beta^\top w_2 \\ &\quad + \rho_0 \left(\sum_{i=1}^r P_i^\top U Q_i + \sum_{i=r+1}^{\min\{m, q\}} |P_i^\top U Q_i| \right) + \lambda_0 \sum_{i=1}^p \left(\beta_i \text{sgn}(\gamma_i) I(\gamma_i \neq 0) + |\beta_i| I(\gamma_i = 0) \right). \end{aligned}$$

Here, $I(\text{Event}) = 1$ if Event happens, and $I(\text{Event}) = 0$ otherwise. $\begin{pmatrix} w_1 \\ w_2 \end{pmatrix} \sim \mathcal{N}(0, \sigma^2 S)$ is a random variable in \mathbb{R}^{mq+p} . $B = P\Sigma Q^\top$ is the singular value decomposition of B , where $\Sigma \in \mathbb{R}^{m \times q}$ is a rectangular diagonal matrix with diagonal elements $\alpha_1 \geq \dots \geq \alpha_r > \alpha_{r+1} = \dots = \alpha_{\min\{m,q\}} = 0$, $r = \text{rank}(B)$, $P = (P_{\cdot 1}, \dots, P_{\cdot m}) \in \mathbb{R}^{m \times m}$, and $Q = (Q_{\cdot 1}, \dots, Q_{\cdot q}) \in \mathbb{R}^{q \times q}$ are orthogonal matrices.

In particular, if $\rho_n = o(\sqrt{n})$ and $\lambda_n = o(\sqrt{n})$, then $\arg \min_{U \in \mathbb{R}^{m \times q}, \beta \in \mathbb{R}^p} F(U, \beta) = (U^*, \beta^*)$ with $[\text{vec}(U^*); \beta^*] = S^{-1}[w_1; w_2] \sim \mathcal{N}(0, \sigma^2 S^{-1})$.

Proof. We define

$$F_n(U, \beta) := \sum_{i=1}^n \left[\left(\varepsilon_i - \frac{1}{\sqrt{n}} \langle X_i, U \rangle - \frac{1}{\sqrt{n}} \langle z_i, \beta \rangle \right)^2 - \varepsilon_i^2 \right] \\ + \rho_n \left(\|B + \frac{1}{\sqrt{n}} U\|_* - \|B\|_* \right) + \lambda_n \left(\|\gamma + \frac{1}{\sqrt{n}} \beta\|_1 - \|\gamma\|_1 \right),$$

for any $(U, \beta) \in \mathbb{R}^{m \times q} \times \mathbb{R}^p$, which is minimized at $\sqrt{n}(\hat{B}_n - B, \hat{\gamma}_n - \gamma)$ by the definition of $(\hat{B}_n, \hat{\gamma}_n)$ and the fact that

$$\left(\varepsilon_i - \frac{1}{\sqrt{n}} \langle X_i, U \rangle - \frac{1}{\sqrt{n}} \langle z_i, \beta \rangle \right)^2 = \left(y_i - \langle X_i, B + \frac{1}{\sqrt{n}} U \rangle - \langle z_i, \gamma + \frac{1}{\sqrt{n}} \beta \rangle \right)^2.$$

By direct computations, we have that

$$\frac{1}{\sqrt{n}} \sum_{i=1}^n \varepsilon_i (\langle X_i, U \rangle + \langle z_i, \beta \rangle) = (\text{vec}(U)^\top \quad \beta^\top) \begin{pmatrix} \frac{1}{\sqrt{n}} \sum_{i=1}^n \varepsilon_i \text{vec}(X_i) \\ \frac{1}{\sqrt{n}} \sum_{i=1}^n \varepsilon_i z_i \end{pmatrix}, \text{ where} \\ \mathbb{E} \left[\begin{pmatrix} \frac{1}{\sqrt{n}} \sum_{i=1}^n \varepsilon_i \text{vec}(X_i) \\ \frac{1}{\sqrt{n}} \sum_{i=1}^n \varepsilon_i z_i \end{pmatrix} \right] = 0, \text{ and } \text{Var} \left[\begin{pmatrix} \frac{1}{\sqrt{n}} \sum_{i=1}^n \varepsilon_i \text{vec}(X_i) \\ \frac{1}{\sqrt{n}} \sum_{i=1}^n \varepsilon_i z_i \end{pmatrix} \right] = \sigma^2 S_n.$$

With the above results, the first term of F_n

$$\sum_{i=1}^n \left[\left(\varepsilon_i - \frac{1}{\sqrt{n}} \langle X_i, U \rangle - \frac{1}{\sqrt{n}} \langle z_i, \beta \rangle \right)^2 - \varepsilon_i^2 \right] \\ = \frac{1}{n} \sum_{i=1}^n (\langle X_i, U \rangle)^2 + \frac{1}{n} \sum_{i=1}^n (\langle z_i, \beta \rangle)^2 + \frac{2}{n} \sum_{i=1}^n \langle X_i, U \rangle \langle z_i, \beta \rangle - \frac{2}{\sqrt{n}} \sum_{i=1}^n \varepsilon_i (\langle X_i, U \rangle + \langle z_i, \beta \rangle) \\ = \text{vec}(U)^\top C_n \text{vec}(U) + \beta^\top D_n \beta + 2 \text{vec}(U)^\top H_n \beta - \frac{2}{\sqrt{n}} \sum_{i=1}^n \varepsilon_i (\langle X_i, U \rangle + \langle z_i, \beta \rangle) \\ \rightarrow \text{vec}(U)^\top C \text{vec}(U) + \beta^\top D \beta + 2 \text{vec}(U)^\top H \beta - 2 \text{vec}(U)^\top w_1 - 2 \beta^\top w_2$$

in distribution. Here $\begin{pmatrix} w_1 \\ w_2 \end{pmatrix} \sim \mathcal{N}(0, \sigma^2 S)$ is the limiting distribution of the random vector $\begin{pmatrix} \frac{1}{\sqrt{n}} \sum_{i=1}^n \varepsilon_i \text{vec}(X_i) \\ \frac{1}{\sqrt{n}} \sum_{i=1}^n \varepsilon_i z_i \end{pmatrix}$ as $n \rightarrow \infty$. For the remaining terms of F_n , we have

$$\lim_{n \rightarrow \infty} \rho_n \left[\|B + \frac{1}{\sqrt{n}} U\|_* - \|B\|_* \right] = \rho_0 \left(\sum_{i=1}^r P_{\cdot i}^\top U Q_{\cdot i} + \sum_{i=r+1}^{\min\{m,q\}} |P_{\cdot i}^\top U Q_{\cdot i}| \right), \\ \lim_{n \rightarrow \infty} \lambda_n \left[\|\gamma + \frac{1}{\sqrt{n}} \beta\|_1 - \|\gamma\|_1 \right] = \lambda_0 \sum_{i=1}^p \left(\beta_i \text{sgn}(\gamma_i) I(\gamma_i \neq 0) + |\beta_i| I(\gamma_i = 0) \right),$$

where the first equation follows from Watson [53, Theorem 1]:

$$\begin{aligned} \lim_{n \rightarrow \infty} \frac{\rho_n}{\sqrt{n}} \frac{\|B + \frac{1}{\sqrt{n}}U\|_* - \|B\|_*}{1/\sqrt{n}} &= \rho_0 \max_{d \in \partial \|\alpha\|_1} \sum_{i=1}^{\min\{m,q\}} d_i P_i^\top U Q_i \\ &= \rho_0 \sum_{i=1}^{\min\{m,q\}} \max_{d_i \in \partial \|\alpha_i\|_1} d_i P_i^\top U Q_i = \rho_0 \left(\sum_{i=1}^r P_i^\top U Q_i + \sum_{i=r+1}^{\min\{m,q\}} |P_i^\top U Q_i| \right), \end{aligned}$$

and the second equation follows from direct computations. Therefore, we have proved that $F_n(U, \beta) \rightarrow F(U, \beta)$ in distribution as $n \rightarrow \infty$. Lastly, given that $F(\cdot, \cdot)$ is strongly convex with $S \succ 0$, guaranteeing a unique minimizer, and $F_n(\cdot, \cdot)$ is convex, we deduce from the work of Geyer [16] that $\sqrt{n}(\hat{B}_n - B, \hat{\gamma}_n - \gamma) \rightarrow \arg \min_{U \in \mathbb{R}^{m \times q}, \beta \in \mathbb{R}^p} F(U, \beta)$ in distribution as $n \rightarrow \infty$. In particular, when $\rho_0 = \lambda_0 = 0$, the minimizer of F is given by

$$(U^*, \beta^*) := \arg \min_{U \in \mathbb{R}^{m \times q}, \beta \in \mathbb{R}^p} F(U, \beta) \text{ with } \begin{pmatrix} \text{vec}(U^*) \\ \beta^* \end{pmatrix} = S^{-1} \begin{pmatrix} w_1 \\ w_2 \end{pmatrix} \sim \mathcal{N}(0, \sigma^2 S^{-1}).$$

The proof is completed. \square

3 A Preconditioned Proximal Point Algorithm

In this section, we design a preconditioned proximal point algorithm (PPA) for solving problem (3). Starting from an initial point $(B^0, \gamma^0) \in \mathbb{R}^{m \times q} \times \mathbb{R}^p$, the preconditioned PPA iteratively computes a sequence $\{(B^k, \gamma^k)\} \subseteq \mathbb{R}^{m \times q} \times \mathbb{R}^p$ as follows:

$$(B^{k+1}, \gamma^{k+1}) \approx \mathbb{J}_k(B^k, \gamma^k) := \arg \min_{B \in \mathbb{R}^{m \times q}, \gamma \in \mathbb{R}^p} G_k(B, \gamma), \quad (8)$$

where

$$G_k(B, \gamma) := G(B, \gamma) + \frac{1}{2\sigma_k} (\|B - B^k\|^2 + \|\gamma - \gamma^k\|^2 + \nu \|X \text{vec}(B) + Z\gamma - X \text{vec}(B^k) - Z\gamma^k\|^2),$$

$\{\sigma_k\}$ is a sequence of nondecreasing positive real numbers, and $\nu > 0$ is a scaling parameter. When $\nu = 0$, it reduces to the classic PPA [44]. We say (8) is a preconditioned PPA iteration due to the last term of G_k . This term is inevitable to derive a smooth unconstrained dual problem of (8), as we will demonstrate shortly. Clearly, an efficient solver for (8) is crucial for the effective implementation of the preconditioned PPA.

We let the convex function $h : \mathbb{R}^n \rightarrow \mathbb{R}$ be defined as

$$h(s) := \hat{\ell}(s, y) \quad (9)$$

and $s^k := X \text{vec}(B^k) + Z\gamma^k$, the minimization problem in (8) can be written equivalently as

$$\begin{aligned} \min_{B \in \mathbb{R}^{m \times q}, \gamma \in \mathbb{R}^p, s \in \mathbb{R}^n} \quad & h(s) + \phi(B) + \psi(\gamma) + \frac{1}{2\sigma_k} \|B - B^k\|^2 + \frac{1}{2\sigma_k} \|\gamma - \gamma^k\|^2 + \frac{\nu}{2\sigma_k} \|s - s^k\|^2 \\ \text{s.t.} \quad & X \text{vec}(B) + Z\gamma - s = 0. \end{aligned} \quad (10)$$

The Lagrangian function associated with (10) is

$$\begin{aligned} \mathcal{L}(B, \gamma, s; \xi) = \quad & h(s) + \phi(B) + \psi(\gamma) + \langle \xi, X \text{vec}(B) + Z\gamma - s \rangle \\ & + \frac{1}{2\sigma_k} \|B - B^k\|^2 + \frac{1}{2\sigma_k} \|\gamma - \gamma^k\|^2 + \frac{\nu}{2\sigma_k} \|s - s^k\|^2 \end{aligned}$$

$$\begin{aligned}
&= h(s) + \phi(B) + \psi(\gamma) + \frac{1}{2\sigma_k} \left(\|B^k\|^2 + \|\gamma^k\|^2 + \nu\|s^k\|^2 \right) \\
&\quad + \frac{1}{2\sigma_k} \|B - B^k + \sigma_k \text{mat}(X^\top \xi)\|^2 + \frac{1}{2\sigma_k} \|\gamma - \gamma^k + \sigma_k Z^\top \xi\|^2 + \frac{\nu}{2\sigma_k} \|s - s^k - \frac{\sigma_k}{\nu} \xi\|^2 \\
&\quad - \frac{1}{2\sigma_k} \left(\|B^k - \sigma_k \text{mat}(X^\top \xi)\|^2 + \|\gamma^k - \sigma_k Z^\top \xi\|^2 + \nu\|s^k + \frac{\sigma_k}{\nu} \xi\|^2 \right),
\end{aligned}$$

for $(B, \gamma, s, \xi) \in \mathbb{R}^{m \times q} \times \mathbb{R}^p \times \mathbb{R}^n \times \mathbb{R}^n$. Therefore, the Lagrangian dual problem of (10) takes the form of

$$\max_{\xi \in \mathbb{R}^n} \left\{ \Phi_k(\xi) := \min_{B \in \mathbb{R}^{m \times q}, \gamma \in \mathbb{R}^p, s \in \mathbb{R}^n} \mathcal{L}(B, \gamma, s; \xi) \right\}. \quad (11)$$

By the definition of Moreau envelope (4), it can be derived that

$$\begin{aligned}
\Phi_k(\xi) &= \frac{1}{\sigma_k} \left[\mathbb{E}_{\sigma_k \phi}(B^k - \sigma_k \text{mat}(X^\top \xi)) + \mathbb{E}_{\sigma_k \psi}(\gamma^k - \sigma_k Z^\top \xi) + \nu \mathbb{E}_{\sigma_k h/\nu}(s^k + \frac{\sigma_k}{\nu} \xi) \right. \\
&\quad \left. - \frac{1}{2} \left(\|B^k - \sigma_k \text{mat}(X^\top \xi)\|^2 + \|\gamma^k - \sigma_k Z^\top \xi\|^2 + \nu\|s^k + \frac{\sigma_k}{\nu} \xi\|^2 \right) \right. \\
&\quad \left. + \frac{1}{2} \left(\|B^k\|^2 + \|\gamma^k\|^2 + \nu\|s^k\|^2 \right) \right].
\end{aligned}$$

An exciting observation is that $\Phi(\cdot)$ is continuously differentiable with Lipschitz continuous gradient, and therefore we can solve problem (11) efficiently via a non-smooth Newton type method for solving the equation $\nabla \Phi_k(\xi) = 0$; see Section 3.1 for details. In addition, the Karush-Kuhn-Tucker (KKT) optimality conditions associated with (10) and (11) are

$$\begin{aligned}
B &= \text{Prox}_{\sigma_k \phi}(B^k - \sigma_k \text{mat}(X^\top \xi)), \quad \gamma = \text{Prox}_{\sigma_k \psi}(\gamma^k - \sigma_k Z^\top \xi), \\
s &= \text{Prox}_{\sigma_k h/\nu}(s^k + \frac{\sigma_k}{\nu} \xi), \quad X \text{vec}(B) + Z\gamma - s = 0.
\end{aligned}$$

Once we obtain an approximate dual solution ξ^{k+1} to (11), we can construct an approximate primal solution $(B^{k+1}, \gamma^{k+1}, s^{k+1})$ to (10) based on the above KKT conditions; see (13).

Algorithm 1 A preconditioned proximal point algorithm for solving (3)

Require: $\nu > 0$, $0 < \sigma_0 \leq \sigma_\infty < \infty$, $\epsilon_k \geq 0$ with $\sum_{k=0}^\infty \epsilon_k < \infty$;

Ensure: an approximate optimal solution (B^{k+1}, γ^{k+1}) to (3).

1: **Initialization:** choose $B^0 \in \mathbb{R}^{m \times q}$, $\gamma^0 \in \mathbb{R}^p$, $k = 0$.

2: **repeat**

3: **Step 1.** Solve via Algorithm 2

$$\xi^{k+1} \approx \arg \max \Phi_k(\xi). \quad (12)$$

4: **Step 2.** Compute

$$\begin{cases} B^{k+1} = \text{Prox}_{\sigma_k \phi}(B^k - \sigma_k \text{mat}(X^\top \xi^{k+1})), \\ \gamma^{k+1} = \text{Prox}_{\sigma_k \psi}(\gamma^k - \sigma_k Z^\top \xi^{k+1}), \\ s^{k+1} = \text{Prox}_{\sigma_k h/\nu}(s^k + \frac{\sigma_k}{\nu} \xi^{k+1}). \end{cases} \quad (13)$$

5: **Step 3.** Update $\sigma_{k+1} \in [\sigma_k, \sigma_\infty]$, $k \leftarrow k + 1$.

6: **until** Stopping criterion is satisfied.

The preconditioned PPA for solving (3) is given in Algorithm 1. For controlling the inexactness in the subproblem (12), we use the following implementable stopping condition (14) based on the duality gap between the subproblem (8) and its dual problem (11):

$$G_k(B^{k+1}, \gamma^{k+1}) - \Phi_k(\xi^{k+1}) \leq \frac{\epsilon_k^2}{2\sigma_k}, \quad \epsilon_k \geq 0, \quad \sum_{k=0}^{\infty} \epsilon_k < \infty. \quad (14)$$

For completeness, we present the global convergence of Algorithm 1 in Theorem 3.1. Its proof follows a similar approach to that of Lin et al. [34, Theorem 2.1], using results of Rockafellar and Wets [45, Exercise 8.8] and Li et al. [31, Theorem 2.3].

Theorem 3.1. *Assume the optimal solution set of problem (3) is nonempty, denoted as Ω . Let $\{(B^k, \gamma^k, \xi^k)\}$ be the sequence generated by Algorithm 1, where the stopping criterion (14) is satisfied at Step 1 of each iteration when solving (12). Then the sequence $\{(B^k, \gamma^k)\}$ is bounded and converges to some $(B^*, \gamma^*) \in \Omega$.*

3.1 A Semismooth Newton Method for Solving the PPA Subproblem

Efficiently solving the subproblem (12) poses a significant implementation challenge for Algorithm 1. Our goal is to devise an efficient semismooth Newton (SSN) method that exhibits at least superlinear convergence. For more details about semismoothness and SSN, see Appendix B. Note that problem (12) can be computed by solving the non-smooth equation $\nabla \Phi_k(\xi) = 0$, where

$$\nabla \Phi_k(\xi) = X \text{vec}(\text{Prox}_{\sigma_k \phi}(B^k - \sigma_k \text{mat}(X^\top \xi))) + Z \text{Prox}_{\sigma_k \psi}(\gamma^k - \sigma_k Z^\top \xi) - \text{Prox}_{\sigma_k h/\nu} \left(s^k + \frac{\sigma_k}{\nu} \xi \right).$$

Define the multifunction $\hat{\partial}^2 \Phi_k$ as: for any $\xi \in \mathbb{R}^n$, $\hat{\partial}^2 \Phi_k(\xi)$ is a multifunction from \mathbb{R}^n to \mathbb{R}^n such that for each $u \in \mathbb{R}^n$,

$$\hat{\partial}^2 \Phi_k(\xi)[u] := \left\{ \begin{array}{l} -\sigma_k X \text{vec}(\mathcal{W}(\text{mat}(X^\top u))) \\ -\sigma_k Z \mathcal{Q} Z^\top u - \frac{\sigma_k}{\nu} \mathcal{M} u \end{array} \left| \begin{array}{l} \mathcal{M} \in \hat{\partial} \text{Prox}_{\sigma_k h/\nu}(s^k + \frac{\sigma_k}{\nu} \xi) \\ \mathcal{W} \in \hat{\partial} \text{Prox}_{\sigma_k \phi}(B^k - \sigma_k \text{mat}(X^\top \xi)) \\ \mathcal{Q} \in \hat{\partial} \text{Prox}_{\sigma_k \psi}(\gamma^k - \sigma_k Z^\top \xi) \end{array} \right. \right\}, \quad (15)$$

where vec and mat are linear maps as defined at the end of the Section 1. Here, we introduce $\hat{\partial} \text{Prox}_f$ as a more computationally efficient alternative to the Clarke generalized Jacobian ∂Prox_f , or even itself, associated with a given closed proper convex function $f : \mathbb{R}^n \rightarrow (-\infty, \infty]$, while ensuring Property A. A multifunction $\hat{\partial} \text{Prox}_f$ is said to satisfy Property A with respect to Prox_f , if (1) it is nonempty, compact valued, and upper-semicontinuous; (2) for any $x \in \mathbb{R}^n$, all the elements in $\hat{\partial} \text{Prox}_f(x)$ are symmetric and positive semidefinite; (3) Prox_f is strongly semismooth with respect to $\hat{\partial} \text{Prox}_f$.

We provide the framework of the SSN for solving (12) in Algorithm 2. In practice, one can choose the parameters as $\mu = 10^{-4}$, $\tau = 0.5$, $\eta = 0.005$ and $\delta = 0.5$.

Theorem 3.2 gives the superlinear convergence of the SSN method, which can be proved using the results of Zhao et al. [59, Proposition 3.3, Theorems 3.4 and 3.5] and Li et al. [29, Theorem 4]. For simplicity, we omit the proof here.

Theorem 3.2. *Assume that the function h in (9) is twice continuously differentiable, and $\hat{\partial} \text{Prox}_{\sigma_k \phi}$ and $\hat{\partial} \text{Prox}_{\sigma_k \psi}$ satisfy Property A with respect to $\text{Prox}_{\sigma_k \phi}$ and $\text{Prox}_{\sigma_k \psi}$, respectively. Let $\{\xi^{k,j}\}$ be the sequence generated by Algorithm 2. Then $\{\xi^{k,j}\}$ converges globally to the unique optimal solution $\bar{\xi}^{k+1}$ of problem (12). Furthermore, the convergence rate is at least superlinear, i.e., for j sufficiently large, $\|\xi^{k,j+1} - \bar{\xi}^{k+1}\| = O(\|\xi^{k,j} - \bar{\xi}^{k+1}\|^{1+\tau})$, where $\tau \in (0, 1]$ is a given parameter in Algorithm 2.*

Algorithm 2 A semismooth Newton method for solving (12)

Require: $\mu \in (0, 0.5)$, $\tau \in (0, 1]$, $\eta \in (0, 1)$, $\delta \in (0, 1)$.

Ensure: an approximate optimal solution ξ^{k+1} to (12).

1: **Initialization:** choose $\xi^{k,0} \in \mathbb{R}^n$, $j = 0$.

2: **repeat**

3: **Step 1.** Select an element $\mathcal{H}_j \in \hat{\partial}^2 \Phi_k(\xi^{k,j})$. Apply the direct method or the conjugate gradient (CG) method to find an approximate solution $d^j \in \mathbb{R}^n$ to

$$\mathcal{H}_j d^j \approx -\nabla \Phi_k(\xi^{k,j}), \quad (16)$$

such that $\|\mathcal{H}_j d^j + \nabla \Phi_k(\xi^{k,j})\| \leq \min(\eta, \|\nabla \Phi_k(\xi^{k,j})\|^{1+\tau})$.

4: **Step 2.** Set $\alpha_j = \delta^{m_j}$, where m_j is the smallest nonnegative integer m for which

$$\Phi_k(\xi^{k,j} + \delta^m d^j) \geq \Phi_k(\xi^{k,j}) + \mu \delta^m \langle \nabla \Phi_k(\xi^{k,j}), d^j \rangle.$$

5: **Step 3.** Set $\xi^{k,j+1} = \xi^{k,j} + \alpha_j d^j$, $\xi^{k+1} = \xi^{k,j+1}$, $j \leftarrow j + 1$.

6: **until** Stopping criterion is satisfied.

Remark 3.3. Here are some comments on Theorem 3.2. First, when the B-subdifferential or Clarke generalized Jacobian of $\text{Prox}_{\sigma_k \phi}$ ($\text{Prox}_{\sigma_k h/\nu}$, $\text{Prox}_{\sigma_k \psi}$) is easy to derive, we can simply take $\hat{\partial} \text{Prox}_{\sigma_k \phi} = \partial_B \text{Prox}_{\sigma_k \phi}$ or $\hat{\partial} \text{Prox}_{\sigma_k \phi} = \partial \text{Prox}_{\sigma_k \phi}$. Second, under the assumption that h is twice continuously differentiable, by Lin et al. [34, Proposition 4.1], we will have the strict concavity of the dual objective function $\Phi_k(\cdot)$, leading to the existence of a unique maximizer for problem (12) and the negative definiteness of all elements in $\hat{\partial}^2 \Phi_k(\bar{\xi}^{k+1})$. In fact, we can also obtain similar convergence results when h is a square root loss under mild assumptions, see [48]. Moreover, for twice continuously differentiable h , $\hat{\partial} \text{Prox}_{\sigma_k h/\nu}$ reduces to one element $\nabla \text{Prox}_{\sigma_k h/\nu}$, and it naturally satisfies Property A.

For many commonly used penalty functions ϕ and ψ , their proximal mappings are strongly semismooth with respect to their (surrogate) generalized Jacobian. We illustrate the application of our algorithm to a specific problem in the following subsection.

3.2 Application on Low Rank and Sparse Regularized Matrix Regression Problems

In this subsection, we consider the application of our algorithmic framework on specific low-rank and sparse regularized matrix regression problems, where

$$h(u) = \frac{1}{2} \|u - y\|^2, \quad u \in \mathbb{R}^n, \quad \phi(B) = \rho \|B\|_*, \quad B \in \mathbb{R}^{m \times q}, \quad \psi(\gamma) = \lambda \|\gamma\|_1, \quad \gamma \in \mathbb{R}^p.$$

We emphasize that our algorithmic framework is quite general as long as the explicit formulae of Prox_ϕ and Prox_ψ are available and their corresponding (surrogate) generalized Jacobians can be well constructed. The following list provides some examples of $\psi(\cdot)$, whose proximal mapping $\text{Prox}_\psi(\cdot)$ along with the (surrogate) generalized Jacobian $\hat{\partial} \text{Prox}_\psi(\cdot)$ are available in the literature. Moreover, the proximal mapping $\text{Prox}_\psi(\cdot)$ is shown to be strongly semismooth, with respect to its (surrogate) generalized Jacobian $\hat{\partial} \text{Prox}_\psi(\cdot)$, enabling their integration into our algorithmic framework.

- Lasso regularizer [49]:

$\psi(\gamma) = \lambda \|\gamma\|_1$, $\lambda > 0$. The proximal mapping and its generalized Jacobian has been well-studied by Li et al. [29, Section 3.3].

- Fused lasso regularizer [50]:
 $\psi(\gamma) = \lambda \|\gamma\|_1 + \lambda' \sum_{i=1}^{p-1} |\gamma_i - \gamma_{(i+1)}|$, $\lambda > 0$, $\lambda' > 0$. The proximal mapping and its generalized Jacobian has been well-studied by Li et al. [30, Section 3].
- Sparse group lasso regularizer [7, 20]:
 $\psi(\gamma) = \lambda \|\gamma\|_1 + \lambda' \sum_{l=1}^g w_l \|\gamma_{G_l}\|$, $\lambda > 0$, $\lambda' > 0$, $w_1, \dots, w_g \geq 0$, and $\{G_1, \dots, G_g\}$ is a disjoint partition of the set $[p]$. It reduces to the group lasso regularizer when $\lambda = 0$. The proximal mapping and its generalized Jacobian has been well-studied by Zhang et al. [58, Proposition 2.1 & Section 3].
- Clustered lasso regularizer [41, 46]:
 $\psi(\gamma) = \lambda \|\gamma\|_1 + \lambda' \sum_{1 \leq i < j \leq p} |\gamma_i - \gamma_j|$, $\lambda > 0$, $\lambda' > 0$. The proximal mapping and its generalized Jacobian has been well-studied by Lin et al. [33, Section 2].
- Exclusive lasso regularizer [24, 61]:
 $\psi(\gamma) = \lambda \sum_{l=1}^g \|\gamma_{G_l} \odot \gamma_{G_l}\|_1^2$, $\lambda > 0$, $w = (w_{G_1}, \dots, w_{G_g}) \in \mathbb{R}_{++}^p$ is a weight vector and $\{G_1, \dots, G_g\}$ is a disjoint partition of the index set $[p]$. The proximal mapping and its generalized Jacobian has been well studied by Lin et al. [34, Section 3].
- Decreasing weighted sorted ℓ_1 -norm (DWSL1) regularizer, also known as sorted ℓ -one penalized estimation (SLOPE) regularizer [3]:
 $\psi(\gamma) = \sum_{i=1}^p \mu_i |\gamma|_{(i)}$, $\mu_1 \geq \dots \geq \mu_p \geq 0$ and $\mu_1 > 0$. Here $|\gamma|_{(i)}$ is the i -th largest component of $|\gamma|$ such that $|\gamma|_{(1)} \geq \dots \geq |\gamma|_{(p)}$ and $|\gamma| \in \mathbb{R}^p$ is obtained from γ by taking the absolute value of its components. The proximal mapping and its generalized Jacobian has been well-studied by Luo et al. [35, Section 2]. Note that Octagonal Shrinkage and Clustering Algorithm for Regression (OSCAR) regularizer $\psi(\gamma) = \lambda \|\gamma\|_1 + \lambda' \max_{i < j} \{|\gamma_i|, |\gamma_j|\}$ is a special case of the DWSL1 regularizer.

Without loss of generality, we assume that $m \leq q$. The next proposition summarizes the formulae for the proximal mapping $\text{Prox}_{\rho\|\cdot\|_*}$ and its Clarke generalized Jacobian $\partial\text{Prox}_{\rho\|\cdot\|_*}$.

Proposition 3.4. *Let $\rho > 0$ and $Y \in \mathbb{R}^{m \times q}$ admit the singular value decomposition*

$$Y = U[\text{Diag}(\sigma_1, \dots, \sigma_m) \ 0]V^\top = U[\text{Diag}(\sigma_1, \dots, \sigma_m) \ 0][V_1 \ V_2]^\top,$$

where $U \in \mathbb{R}^{m \times m}$, $V = [V_1 \ V_2] \in \mathbb{R}^{q \times q}$ are orthogonal matrices, $V_1 \in \mathbb{R}^{q \times m}$, $V_2 \in \mathbb{R}^{q \times (q-m)}$, and $\sigma_1 \geq \sigma_2 \geq \dots \geq \sigma_m \geq 0$ are the singular values of Y . Then we have the following conclusions.

(a) *The proximal mapping associated with $\rho\|\cdot\|_*$ at Y can be computed as*

$$\text{Prox}_{\rho\|\cdot\|_*}(Y) = U[\text{Diag}((\sigma_1 - \rho)_+, \dots, (\sigma_m - \rho)_+) \ 0]V^\top.$$

(b) *The function $\text{Prox}_{\rho\|\cdot\|_*}(\cdot)$ is strongly semismooth everywhere in $\mathbb{R}^{m \times q}$ with respect to $\partial\text{Prox}_{\rho\|\cdot\|_*}(\cdot)$.*

(c) *Define the index sets*

$$\begin{aligned} \alpha &= \{1, \dots, m\}, \quad \gamma = \{m+1, \dots, 2m\}, \quad \beta = \{2m+1, \dots, m+q\}, \\ \alpha_1 &= \{i \in [m] \mid \sigma_i > \rho\}, \quad \alpha_2 = \{i \in [m] \mid \sigma_i = \rho\}, \quad \alpha_3 = \{i \in [m] \mid \sigma_i < \rho\}. \end{aligned}$$

We can construct one element $\mathcal{W} \in \partial\text{Prox}_{\rho\|\cdot\|_*}(Y)$, where $\mathcal{W} : \mathbb{R}^{m \times q} \rightarrow \mathbb{R}^{m \times q}$ is defined as

$$\mathcal{W}(H) = U \left[\left(\Gamma_{\alpha\alpha} \odot \left(\frac{H_1 + H_1^\top}{2} \right) + \Gamma_{\alpha\gamma} \odot \left(\frac{H_1 - H_1^\top}{2} \right) \right) V_1^\top + (\Gamma_{\alpha\beta} \odot H_2) V_2^\top \right],$$

for $H \in \mathbb{R}^{m \times q}$. Here $H_1 = U^\top H V_1$, $H_2 = U^\top H V_2$, $\Gamma_{\alpha\alpha} \in \mathbb{S}^m$, $\Gamma_{\alpha\gamma} \in \mathbb{S}^m$, $\Gamma_{\alpha\beta} \in \mathbb{R}^{m \times (q-m)}$ are defined as

$$\Gamma_{\alpha\alpha}^0 = \begin{pmatrix} 1_{\alpha_1\alpha_1} & 1_{\alpha_1\alpha_2} & \tau_{\alpha_1\alpha_3} \\ 1_{\alpha_2\alpha_1} & 0 & 0 \\ \tau_{\alpha_1\alpha_3}^\top & 0 & 0 \end{pmatrix}, \quad \Gamma_{\alpha\gamma} = \begin{pmatrix} \omega_{\alpha_1\alpha_1} & \omega_{\alpha_1\alpha_2} & \omega_{\alpha_1\alpha_3} \\ \omega_{\alpha_1\alpha_2}^\top & 0 & 0 \\ \omega_{\alpha_1\alpha_3}^\top & 0 & 0 \end{pmatrix}, \quad \Gamma_{\alpha\beta} = \begin{pmatrix} \mu_{\alpha_1\beta} \\ 0 \end{pmatrix},$$

with $\tau_{\alpha_1\alpha_3} \in \mathbb{R}^{|\alpha_1| \times |\alpha_3|}$, $\omega_{\alpha_1\alpha} \in \mathbb{R}^{|\alpha_1| \times m}$, $\mu_{\alpha_1\bar{\beta}} \in \mathbb{R}^{|\alpha_1| \times (q-m)}$ defined as

$$\begin{aligned}\tau_{ij} &= \frac{\sigma_i - \rho}{\sigma_i - \sigma_j}, \quad \text{for } i \in \alpha_1, j \in \alpha_3, \\ \omega_{ij} &= \frac{\sigma_i - \rho + (\sigma_j - \rho)_+}{\sigma_i + \sigma_j}, \quad \text{for } i \in \alpha_1, j \in \alpha, \\ \mu_{ij} &= \frac{\sigma_i - \rho}{\sigma_i}, \quad \text{for } i \in \alpha_1, j \in \bar{\beta} := \{1, \dots, q - m\}.\end{aligned}$$

Proof. (a) follows from [4, 36]. (b) follows from [22, Theorem 2.1]. (c) follows from [55, Lemma 2.3.6, Proposition 2.3.7] and the fact that

$$\partial_B \text{Prox}_{\rho\|\cdot\|_*}(Y) \subseteq \partial \text{Prox}_{\rho\|\cdot\|_*}(Y) = \text{conv}(\partial_B \text{Prox}_{\rho\|\cdot\|_*}(Y))$$

for any $Y \in \mathbb{R}^{m \times q}$. \square

In addition to the above formulae, we need the following standard results for constructing one element in the set (15):

$$\begin{aligned}\text{Prox}_{\sigma_k h/\nu}(u) &= \frac{u + \frac{\sigma_k}{\nu}y}{1 + \frac{\sigma_k}{\nu}}, \quad \nabla \text{Prox}_{\sigma_k h/\nu}(u) = \frac{1}{1 + \frac{\sigma_k}{\nu}}I_n, \\ (\text{Prox}_{\sigma_k \psi}(\gamma))_i &= \text{sgn}(\gamma_i)(|\gamma_i| - \sigma_k \lambda)_+, \quad i \in [p], \\ \partial \text{Prox}_{\sigma_k \psi}(\gamma) &= \left\{ \text{Diag}(w) \begin{cases} w_i = 0 & \text{if } |\gamma_i| < \sigma_k \lambda, \\ w_i \in [0, 1] & \text{if } |\gamma_i| = \sigma_k \lambda, i \in [p] \\ w_i = 1 & \text{if } |\gamma_i| > \sigma_k \lambda, \end{cases} \right\}.\end{aligned}$$

Therefore, with one element $\mathcal{W} \in \partial \text{Prox}_{\sigma_k \rho\|\cdot\|_*}(B^k - \sigma_k \text{mat}(X^\top \xi))$ constructed via Proposition 3.4, we can construct one element $\mathcal{H} : \mathbb{R}^n \rightarrow \mathbb{R}^n$ in the set $\hat{\partial}^2 \Phi_k(\xi)$ such that for each $u \in \mathbb{R}^n$:

$$\begin{aligned}\mathcal{H}u &:= -\sigma_k X \text{vec}(\mathcal{W}(\text{mat}(X^\top u))) - \sigma_k Z D Z^\top u - \frac{\sigma_k}{\nu + \sigma_k}u \\ &= -\sigma_k X \text{vec}(\mathcal{W}(\text{mat}(X^\top u))) - \sigma_k Z_{\mathcal{A}} Z_{\mathcal{A}}^\top u - \frac{\sigma_k}{\nu + \sigma_k}u,\end{aligned}$$

where $D \in \mathbb{S}^p$ is a diagonal matrix with its (i, i) -th element being 1 if $i \in \mathcal{A} := \{i \in [p] \mid |(\gamma^k - \sigma_k Z^\top \xi)_i| > \sigma_k \lambda\}$ and 0 otherwise, and $Z_{\mathcal{A}}$ is the matrix consisting of the columns of Z indexed by \mathcal{A} . This reflects the second-order sparsity.

4 Numerical Experiments

In this section, we conduct extensive numerical experiments with two objectives. First, in Section 4.1, we assess and compare the empirical performances, in terms of prediction and estimation accuracy, of various regularized models in the form of (3) that employ different penalty functions ϕ and ψ . This also shows the practical and general applicability of the PPDNA, accommodating penalty functions of various forms. Second, in Section 4.2, we evaluate and contrast the efficiency of different optimization algorithms in terms of computational time, which aims to highlight the superior efficiency of the PPDNA among other state-of-the-art algorithms. We take the squared loss function in (3). All experiments were conducted using MATLAB 2019b on a computer with an i7-860, 2.80 GHz CPU, and 16 GB of RAM.

4.1 Comparison of Empirical Performance

We evaluate the empirical performances of various estimators obtained from (3), each corresponding to a specific combination of penalty functions $\phi(B)$ and $\psi(\gamma)$. These penalties are as follows: (i) $\rho \|\text{vec}(B)\|_1 + \lambda \|\gamma\|_1$, referred to as VML, where the estimator is obtained by applying the lasso penalty after vectorizing the matrix variable; (ii) $\rho \|B\|_* + \lambda \|\gamma\|_1$, referred to as NL as it includes the nuclear norm and lasso penalty; (iii) $\rho \|B\|_* + \lambda \|\gamma\|_1 + \lambda' \sum_{i=1}^{p-1} |\gamma_i - \gamma_{i+1}|$, referred to as NFL as it includes the nuclear norm and fused lasso penalty; (iv) $\rho \|B\|_* + \lambda \|\gamma\|_1 + \lambda' \sum_{l=1}^g \sqrt{w_l} \|\gamma_{G_l}\|_2$, referred to as NSGL as it includes the nuclear norm and sparse group lasso penalty, where $w_l > 0$ is the weight for the l -th group, G_l 's denote the group index sets forming a partition of $[p]$, and γ_{G_l} is the subvector of γ restricted to G_l .

In Section 4.1.1, we explore on various two-dimensional geometrically shaped true matrix coefficient B following Zhou and Li [60, Section 5.1]. Additionally, in Section 4.1.2, we simulate on true matrix coefficient B with varying ranks and non-sparsity levels (the percentage of nonzero elements) following Zhou and Li [60, Section 5.2]. As a given information for NSGL estimators, we construct the group structure simply by dividing the index set $[p]$ into adjacent groups G_1, \dots, G_g with an approximately equal group size of around p/g . The true vector coefficient γ is generated using one of the following three schemes, each designed to exhibit specific characteristics:

- (S1) Sparsity: we set $g = 10$ and randomly choose an element in each group of γ to be 5, while the rest are 0;
- (S2) Local constancy: we set $g = 10$ and assign the first ten elements in each group of γ to be 1, with the remaining elements being 0;
- (S3) Group structure: we set $g = 20$. For the first ten groups of γ , we alternate the first ten elements in each group between 1 and -1 , that is, $(1, -1, 1, -1, \dots, 1, -1)$, with the remaining elements being 0.

We choose the tuning parameters to be

$$\rho = \alpha_1 \|\text{mat}(X^\top y)\|_2, \quad \lambda = \lambda' = \alpha_2 \|Z^\top y\|_\infty, \quad (17)$$

for NL, NFL and NSGL, and

$$\rho = \alpha_3 \|X^\top y\|_\infty, \quad \lambda = \alpha_4 \|Z^\top y\|_\infty,$$

for VML. Here, $0 < \alpha_1, \alpha_2, \alpha_3, \alpha_4 < 1$. More discussions on the selection of λ and λ' are given in Appendix C.2. On a training set of size 300, we search a large grid of values of $\alpha_1, \alpha_2, \alpha_3, \alpha_4$ in the range of 10^{-3} to 1 with 20 equally divided grid points on the \log_{10} scale, and then select the parameters yielding the best predicting root-mean-square error (RMSE) on a validation data with a large sample size of 3000. Lastly, a testing data set of size 300 serves to evaluate the chosen model's generalization ability on unseen data. Similar procedure is also adopted by Li et al. [27, Section 5.1].

To compare the empirical performances of different estimators, we consistently apply our proposed PPDNA for solving problem (3) and derive the corresponding estimators. Specifically, we initialize the algorithm with zeros and terminate it when either the KKT residual is sufficiently small

$$\eta_{\text{KKT}} := \max\{R_p, R_d, R_c\} < 10^{-6}, \quad (18)$$

or the number of iterations reaches 100, where the formulae for R_p , R_d and R_c are in (31).

We assess the empirical performance of our method from two aspects: parameter estimation and prediction accuracy based on 100 repetitions. For the former, we compute the RMSE of B and γ based on the estimated (B^*, γ^*) , denoted as Error- B and Error- γ . For the latter, we use the testing data set to evaluate the prediction error measured by the RMSE of the response y ,

denoted as RMSE- y . Specifically,

$$\text{RMSE-}y = \frac{\|y_{\text{test}} - y_{\text{test}}^*\|}{\sqrt{n}}, \quad \text{Error-}B = \frac{\|B - B^*\|_F}{\sqrt{mq}}, \quad \text{Error-}\gamma = \frac{\|\gamma - \gamma^*\|}{\sqrt{p}},$$

where B and γ are the true matrix and vector coefficients, respectively, B^* and γ^* are the corresponding estimated values, and $y_{\text{test}}^* = X_{\text{test}} \text{vec}(B^*) + Z_{\text{test}} \gamma^*$ with $\{(y_{\text{test}}, X_{\text{test}}, Z_{\text{test}})\}$ being the testing data set.

4.1.1 Two Dimensional Shapes

We set the problem dimensions as follows: $m = 64$, $q = 64$, and $p = 1000$, with a sample size of $n = 300$. The true matrix coefficient $B \in \{0, 1\}^{m \times q}$ is binary, and its true signal region forms a two dimensional shape (square, triangle, circle, heart, see Appendix C.3). The true vector coefficient $\gamma \in \mathbb{R}^p$ is generated using schemes (S1), (S2), and (S3). To generate the data, we randomly sample $\{(X_i, z_i) \in \mathbb{R}^{m \times q} \times \mathbb{R}^p, i \in [n]\}$ such that each entry follows a standard normal distribution. The response $y_i \in \mathbb{R}$ also follows a normal distribution with mean $\langle X_i, B \rangle + \langle z_i, \gamma \rangle$ and variance 1.

Table 1: Comparison of the four estimators VML, NL, NFL, and NSGL of different true coefficients B and γ , based on 100 replications. Standard deviations are provided in parentheses below. The best value is highlighted in bold.

		RMSE- y				Error- B				Error- γ			
B	γ	VML	NL	NFL	NSGL	VML	NL	NFL	NSGL	VML	NL	NFL	NSGL
Square	S1	16.81 (0.81)	6.58 (1.33)	7.98 (1.47)	17.98 (0.84)	0.23 (0.00)	0.09 (0.02)	0.11 (0.02)	0.19 (0.01)	0.24 (0.03)	0.09 (0.03)	0.13 (0.03)	0.42 (0.01)
	S2	18.00 (0.69)	14.35 (0.80)	10.91 (1.20)	14.30 (0.82)	0.23 (0.00)	0.16 (0.01)	0.14 (0.02)	0.17 (0.01)	0.32 (0.00)	0.31 (0.01)	0.21 (0.02)	0.30 (0.01)
	S3	17.92 (0.73)	14.47 (0.81)	14.60 (0.75)	13.74 (0.77)	0.23 (0.00)	0.17 (0.01)	0.17 (0.01)	0.16 (0.01)	0.32 (0.00)	0.31 (0.01)	0.32 (0.00)	0.29 (0.01)
	S1	12.72 (0.64)	9.60 (0.73)	10.34 (0.78)	16.76 (0.64)	0.18 (0.00)	0.13 (0.01)	0.14 (0.01)	0.17 (0.01)	0.19 (0.02)	0.14 (0.02)	0.17 (0.02)	0.41 (0.01)
	S2	15.09 (0.59)	13.97 (0.62)	11.78 (0.74)	13.99 (0.68)	0.18 (0.00)	0.16 (0.01)	0.15 (0.01)	0.16 (0.01)	0.31 (0.01)	0.31 (0.01)	0.23 (0.02)	0.30 (0.00)
	S3	15.06 (0.56)	13.99 (0.67)	14.20 (0.64)	13.87 (0.73)	0.18 (0.00)	0.16 (0.01)	0.16 (0.01)	0.16 (0.01)	0.31 (0.00)	0.31 (0.00)	0.32 (0.00)	0.30 (0.01)
Circle	S1	11.12 (0.56)	7.84 (0.69)	8.60 (0.83)	16.19 (0.66)	0.15 (0.00)	0.11 (0.01)	0.11 (0.01)	0.16 (0.00)	0.16 (0.02)	0.11 (0.02)	0.14 (0.02)	0.40 (0.01)
	S2	14.06 (0.57)	13.29 (0.69)	9.94 (0.79)	12.86 (0.66)	0.16 (0.00)	0.14 (0.01)	0.12 (0.01)	0.14 (0.01)	0.31 (0.00)	0.30 (0.01)	0.19 (0.02)	0.29 (0.01)
	S3	14.06 (0.55)	13.52 (0.64)	13.36 (0.59)	12.53 (0.62)	0.16 (0.00)	0.15 (0.01)	0.14 (0.01)	0.14 (0.01)	0.31 (0.01)	0.31 (0.01)	0.32 (0.00)	0.28 (0.01)
	S1	12.59 (0.65)	9.21 (0.81)	9.78 (0.95)	17.02 (0.88)	0.17 (0.00)	0.13 (0.01)	0.13 (0.01)	0.17 (0.01)	0.18 (0.03)	0.14 (0.02)	0.16 (0.03)	0.42 (0.01)
	S2	14.97 (0.58)	14.01 (0.73)	11.25 (0.84)	13.50 (0.65)	0.18 (0.00)	0.15 (0.01)	0.14 (0.01)	0.15 (0.01)	0.31 (0.01)	0.31 (0.01)	0.22 (0.02)	0.30 (0.00)
	S3	15.10 (0.66)	13.78 (0.73)	14.07 (0.71)	13.51 (0.73)	0.18 (0.00)	0.15 (0.01)	0.15 (0.01)	0.15 (0.01)	0.32 (0.00)	0.31 (0.01)	0.32 (0.00)	0.29 (0.01)

In Table 1, we present the RMSE- y , Error- B , and Error- γ of the four estimators VML, NL, NFL, and NSGL. These estimators are evaluated under various scenarios where the true coefficients B and γ are generated differently. From Table 1, we observe that the VML estimator consistently fails to achieve the best performance. This observation suggests that the nuclear norm penalty function is more suitable than the element-wise ℓ_1 norm penalty function for B , especially for certain shapes in this context. Moreover, when the true vector coefficient is generated using scheme (S1), the NL estimator demonstrates the best performances in all cases. Similarly, for scheme (S2) (and (S3)), the NFL (and NSGL) estimator generally exhibits the best performance. We may conclude that the empirical performance of the regularized regression model (3) heavily depends on the selection of appropriate penalty functions to capture the characteristics of the true coefficients. Our results also demonstrate the versatility of our PPDNA for solving (3) with various penalties.

For illustrative purposes, we display in Figure 1 the true coefficients and the estimated coefficients by VML, NL, NFL, and NSGL for a square shaped B . We can see from the second column of Figure 1 that the VML estimator exhibits the least effective visual recovery. Notably, in the second row of Figure 1, the NFL estimator demonstrates the best recovery of truth, while in the third row the NSGL estimator achieves the best recovery.

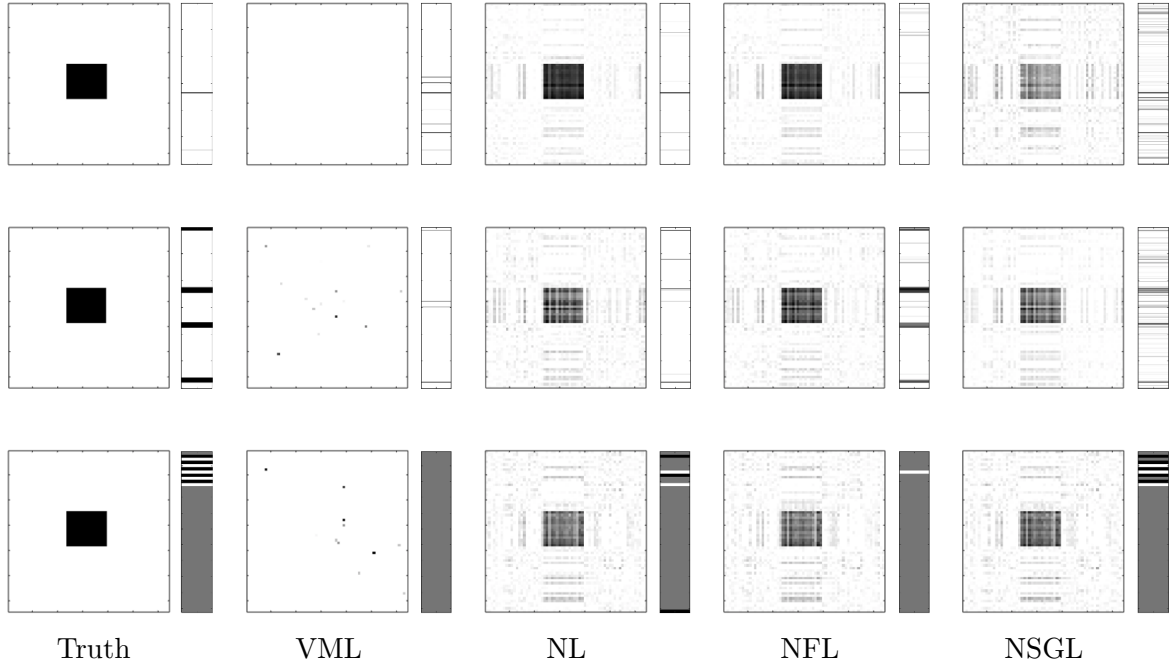


Figure 1: Comparison of the four estimators VML, NL, NFL, and NSGL under square shaped B and different γ generating schemes (S1), (S2), and (S3) from top to bottom rows. In each subgraph, the left square depicts the matrix coefficients, while the right rectangle depicts the vector coefficients. For clarity, segment from 100 to 400 of estimated vector coefficients is displayed for (S1) and (S2), while for (S3), the segment is from 210 to 260 (5th group). For every estimated matrix coefficients, we set the color limit to be 0 and 1, that is, entries with non-positive values are mapped to white, entries with values greater than 1 are mapped to black, and entries with values between 0 and 1 are uniformly mapped to a color scale ranging from white to black. For estimated vector coefficients, we set the color limit to be 0 and 1 for (S1) and (S2), while for (S3), we map entries whose absolute values are smaller than 0.2 to gray, and the entries that are greater than 0.2 to black, and those less than -0.2 to white to highlight the group structure.

4.1.2 Synthetic Data

We set the problem dimensions as follows: $m = 50$, $q = 50$, and $p = 1000$, with a sample size of $n = 300$. We generate the true matrix coefficient B as the product of two matrices $B = B_1 B_2^T$, where $B_1 \in \mathbb{R}^{m \times r}$, $B_2 \in \mathbb{R}^{q \times r}$, and r controls the rank of B . Each entry of B_1 and B_2 is independently generated from a Bernoulli distribution with probability of one equal to $\sqrt{1 - (1 - s)^{1/r}}$. We can deduce that the non-sparsity level (the percentage of nonzero elements) of B is expected to be s . We choose the rank $r = 1, 2, 4$, and the non-sparsity level $s = 0.1, 0.2, 0.4$. The true vector coefficient γ and samples (y_i, X_i, z_i) are generated in the same manner as described in Section 4.1.1.

Tables 2, 3, and 4 present the RMSE- y , Error- B , and Error- γ of the four estimators VML, NL, NFL, and NSGL evaluated under various scenarios. These scenarios involve different ranks r and non-sparsity levels s for the true coefficients B , while γ is generated using schemes (S1), (S2), and (S3). From Tables 2 to 4, several observations can be made as follows. First, the VML estimator has the highest RMSE- y , Error- B , Error- γ in all scenarios, which implies the inferiority of the ℓ_1 penalty $\|\text{vec}(B)\|_1$ compared to the nuclear norm penalty $\|B\|_*$. Second, when γ is generated using scheme (S1), the NL estimator consistently demonstrates the lowest error in the estimation of B , γ and in the prediction of y . Similarly, the NFL estimator has the lowest error in most cases in Table 3 where γ is generated using scheme (S2), and the NSGL estimator generally achieves the lowest error in Table 4 where γ is generated using scheme (S3). Again, we conclude that the choice of penalty functions is contingent on the specific characteristics of predictors. And our simulations reflect the versatility and generality of the PPDNA.

Table 2: Comparison of the four estimators VML, NL, NFL, and NSGL under B with different ranks r and non-sparsity levels s , together with γ generating schemes (S1), based on 100 replications.

		RMSE- y				Error- B				Error- γ				
s	r	VML	NL	NFL	NSGL	VML	NL	NFL	NSGL	VML	NL	NFL	NSGL	
0.1	1	17.799 (2.876)	3.478 (0.868)	4.067 (1.112)	17.210 (1.207)	0.317 (0.048)	0.058 (0.015)	0.067 (0.019)	0.221 (0.023)	0.253 (0.050)	0.052 (0.016)	0.066 (0.021)	0.417 (0.012)	
	2	18.510 (3.165)	11.167 (1.885)	12.950 (2.218)	19.595 (1.753)	0.323 (0.053)	0.197 (0.032)	0.218 (0.036)	0.276 (0.034)	0.279 (0.059)	0.162 (0.036)	0.215 (0.046)	0.437 (0.019)	
	4	18.838 (2.555)	15.686 (2.099)	16.387 (2.164)	20.605 (1.580)	0.328 (0.040)	0.274 (0.032)	0.279 (0.032)	0.302 (0.030)	0.285 (0.049)	0.234 (0.046)	0.267 (0.047)	0.440 (0.013)	
	0.2	1	24.939 (3.307)	3.555 (0.899)	4.787 (1.443)	18.813 (1.336)	0.450 (0.055)	0.060 (0.016)	0.080 (0.024)	0.265 (0.024)	0.348 (0.050)	0.051 (0.015)	0.078 (0.026)	0.426 (0.012)
		2	27.117 (3.524)	15.472 (2.097)	17.316 (2.295)	22.921 (1.642)	0.483 (0.064)	0.273 (0.037)	0.296 (0.039)	0.354 (0.034)	0.379 (0.057)	0.219 (0.041)	0.277 (0.047)	0.454 (0.014)
		4	27.792 (2.956)	21.971 (2.478)	23.150 (2.413)	25.708 (1.859)	0.496 (0.049)	0.390 (0.039)	0.398 (0.038)	0.415 (0.035)	0.393 (0.046)	0.317 (0.054)	0.369 (0.049)	0.471 (0.014)
0.4	1	35.279 (2.972)	3.903 (1.220)	5.714 (2.205)	20.764 (1.598)	0.640 (0.050)	0.066 (0.022)	0.096 (0.038)	0.307 (0.031)	0.457 (0.047)	0.055 (0.019)	0.092 (0.038)	0.440 (0.012)	
	2	40.383 (4.272)	22.738 (2.760)	22.800 (2.719)	26.603 (1.954)	0.740 (0.075)	0.395 (0.046)	0.394 (0.045)	0.440 (0.037)	0.488 (0.052)	0.349 (0.053)	0.354 (0.053)	0.470 (0.013)	
	4	43.102 (4.151)	30.262 (2.629)	31.635 (2.276)	31.792 (2.372)	0.809 (0.074)	0.546 (0.042)	0.559 (0.040)	0.558 (0.041)	0.483 (0.034)	0.411 (0.041)	0.471 (0.020)	0.484 (0.011)	

Table 3: Comparison of the four estimators VML, NL, NFL, and NSGL under B with different ranks r and non-sparsity levels s , together with γ generating schemes (S2), based on 100 replications.

s	r	RMSE- y				Error- B				Error- γ			
		VML	NL	NFL	NSGL	VML	NL	NFL	NSGL	VML	NL	NFL	NSGL
0.1	1	18.489 (2.348)	14.018 (1.253)	7.982 (1.764)	13.221 (1.043)	0.310 (0.053)	0.189 (0.023)	0.121 (0.027)	0.184 (0.021)	0.315 (0.002)	0.326 (0.016)	0.160 (0.038)	0.299 (0.008)
	2	19.281 (2.404)	15.860 (1.373)	13.931 (1.954)	16.151 (1.577)	0.326 (0.052)	0.246 (0.030)	0.228 (0.033)	0.251 (0.033)	0.317 (0.006)	0.314 (0.008)	0.248 (0.028)	0.314 (0.011)
	4	19.335 (1.919)	17.490 (1.505)	16.530 (1.627)	17.383 (1.426)	0.330 (0.043)	0.286 (0.032)	0.281 (0.031)	0.285 (0.031)	0.318 (0.007)	0.319 (0.007)	0.274 (0.014)	0.313 (0.002)
0.2	1	24.530 (2.551)	14.715 (1.004)	10.639 (2.056)	14.030 (1.095)	0.448 (0.053)	0.217 (0.020)	0.166 (0.034)	0.208 (0.021)	0.316 (0.000)	0.316 (0.001)	0.208 (0.038)	0.299 (0.005)
	2	26.568 (2.910)	18.947 (1.561)	17.431 (1.666)	18.446 (1.485)	0.488 (0.059)	0.316 (0.030)	0.301 (0.030)	0.312 (0.028)	0.316 (0.001)	0.328 (0.011)	0.277 (0.017)	0.309 (0.004)
	4	26.840 (2.557)	21.835 (1.751)	21.761 (1.843)	21.828 (1.752)	0.493 (0.055)	0.385 (0.035)	0.385 (0.036)	0.385 (0.035)	0.317 (0.003)	0.316 (0.000)	0.310 (0.020)	0.316 (0.001)
0.4	1	33.062 (2.592)	15.526 (1.165)	11.578 (2.086)	15.175 (1.083)	0.628 (0.044)	0.238 (0.024)	0.184 (0.035)	0.234 (0.022)	0.319 (0.004)	0.314 (0.007)	0.218 (0.035)	0.306 (0.004)
	2	38.925 (3.496)	21.139 (1.640)	20.426 (1.903)	21.380 (1.820)	0.750 (0.065)	0.373 (0.031)	0.364 (0.034)	0.377 (0.034)	0.326 (0.013)	0.316 (0.001)	0.297 (0.019)	0.323 (0.010)
	4	41.099 (4.182)	27.812 (2.018)	27.806 (2.013)	27.806 (2.025)	0.792 (0.081)	0.517 (0.039)	0.517 (0.039)	0.517 (0.039)	0.316 (0.000)	0.316 (0.000)	0.316 (0.001)	0.316 (0.001)

Table 4: Comparison of the four estimators VML, NL, NFL, and NSGL under B with different ranks r and non-sparsity levels s , together with γ generating schemes (S3), based on 100 replications.

s	r	RMSE- y				Error- B				Error- γ			
		VML	NL	NFL	NSGL	VML	NL	NFL	NSGL	VML	NL	NFL	NSGL
0.1	1	18.195 (2.120)	13.311 (0.762)	13.618 (0.788)	12.499 (0.842)	0.304 (0.048)	0.182 (0.018)	0.186 (0.018)	0.174 (0.019)	0.316 (0.001)	0.306 (0.005)	0.315 (0.005)	0.281 (0.008)
	2	18.664 (2.017)	15.556 (1.187)	15.659 (1.182)	15.099 (1.271)	0.316 (0.042)	0.241 (0.024)	0.242 (0.024)	0.237 (0.025)	0.316 (0.001)	0.311 (0.005)	0.316 (0.000)	0.297 (0.009)
	4	19.700 (1.908)	17.838 (1.402)	17.790 (1.388)	17.516 (1.460)	0.335 (0.040)	0.291 (0.029)	0.290 (0.029)	0.289 (0.029)	0.317 (0.004)	0.315 (0.004)	0.316 (0.000)	0.306 (0.008)
0.2	1	24.181 (2.558)	14.593 (0.914)	14.638 (0.855)	13.747 (0.893)	0.440 (0.056)	0.215 (0.020)	0.213 (0.020)	0.204 (0.019)	0.318 (0.005)	0.310 (0.007)	0.315 (0.003)	0.291 (0.006)
	2	25.944 (2.899)	18.245 (1.420)	18.276 (1.430)	18.073 (1.464)	0.477 (0.059)	0.306 (0.030)	0.306 (0.030)	0.305 (0.030)	0.327 (0.011)	0.315 (0.003)	0.316 (0.001)	0.308 (0.005)
	4	27.183 (2.585)	22.197 (1.790)	22.205 (1.794)	22.559 (1.961)	0.507 (0.050)	0.396 (0.032)	0.397 (0.032)	0.401 (0.034)	0.316 (0.000)	0.316 (0.001)	0.316 (0.000)	0.332 (0.013)
0.4	1	33.195 (2.948)	15.414 (1.099)	15.583 (1.127)	14.717 (1.136)	0.631 (0.056)	0.237 (0.022)	0.239 (0.023)	0.227 (0.022)	0.319 (0.004)	0.312 (0.003)	0.316 (0.000)	0.293 (0.007)
	2	38.469 (3.454)	21.212 (1.843)	21.239 (1.841)	21.163 (1.835)	0.743 (0.062)	0.374 (0.035)	0.374 (0.035)	0.373 (0.035)	0.332 (0.015)	0.316 (0.000)	0.317 (0.002)	0.315 (0.002)
	4	42.049 (3.872)	28.281 (2.282)	28.281 (2.282)	28.313 (2.288)	0.817 (0.073)	0.528 (0.039)	0.528 (0.039)	0.529 (0.039)	0.316 (0.000)	0.316 (0.000)	0.316 (0.000)	0.316 (0.001)

4.2 Comparison of Algorithm Efficiency

This subsection aims to reveal the relative performance and applicability of the PPDNA for solving (3), highlighting its potential efficiency over established methods such as the ADMM and the Nesterov algorithm. For illustrative purpose, we choose the penalty function to be $\phi(B) + \psi(\gamma) = \rho\|B\|_* + \lambda\|\gamma\|_1$, resulting NL estimators. Other forms of ψ yield quite similar results in terms of the performance of algorithm efficiency.

We compare the efficiency of our PPDNA with two state-of-the-art algorithms: the Nesterov algorithm implemented by Zhou and Li [60] and the alternating direction method of multipliers (ADMM), of which the details are given in Appendix C.1. It is worth noting that the Nesterov algorithm presented by Zhou and Li [60] was primarily designed for estimating the low rank matrix coefficient B without regularization on the vector coefficient γ ($\lambda = 0$). In our experiments, we implemented the Nesterov algorithm [60, Algorithm 1] from <https://hua-zhou.github.io/SparseReg> and <https://hua-zhou.github.io/TensorReg>. We implemented the ADMM by ourselves, see Appendix C.1 for more details. We note that there is an ADMM type method [27, Algorithm 1] for obtaining the NFL estimator, while their codes are not available.

For each instance, we run the PPDNA to a high accuracy, terminating after a maximum of 50 iterations or when $\eta_{\text{KKT}} < 10^{-10}$ (see (18)), and use the resulting solution as a benchmark. We denote the benchmark objective function value of (3) as obj^* . For the objective function value of one method, denoted as obj , we compute the relative objective function value

$$R_{\text{obj}} := (\text{obj} - \text{obj}^*) / (1 + |\text{obj}^*|). \quad (19)$$

We initialize each algorithm with zero and set a maximum computational time of one hour. For the PPDNA, we terminate execution when either $R_{\text{obj}} < 10^{-10}$ or the number of iterations reaches 50. While for the ADMM and the Nesterov algorithm, termination occurs when either $R_{\text{obj}} < 10^{-10}$ or the number of iterations reaches 500,000.

As mentioned before, the Nesterov algorithm [60, Algorithm 1] does not support regularization on the vector coefficient γ (that is, it is only capable in the case when $\lambda = 0$). In order to include the Nesterov algorithm [60, Algorithm 1] into comparison, we first use the regularization setting:

$$\rho = \alpha\|\text{mat}(X^\top y)\|_2 \text{ with } 0 < \alpha < 1, \lambda = 0, \quad (20)$$

and compare the three algorithms PPDNA, ADMM, and Nesterov algorithm under this setting. Additionally, we also compare PPDNA and ADMM under the setting as in (17):

$$\rho = \alpha_1\|\text{mat}(X^\top y)\|_2, \quad \lambda = \alpha_2\|Z^\top y\|_\infty, \text{ with } \alpha_1, \alpha_2 \in (0, 1). \quad (21)$$

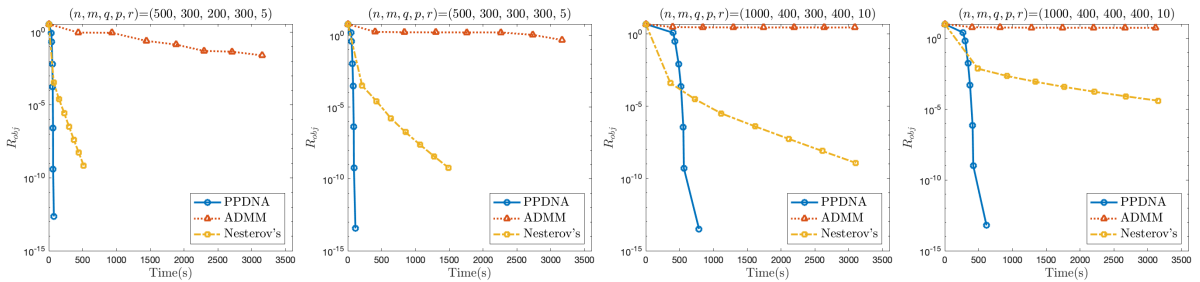


Figure 2: Time vs. R_{obj} (see (19)) of PPDNA, ADMM, and Nesterov algorithm on synthetic data. The penalty parameters are taken from Table 5 with asterisks (*).

4.2.1 Synthetic Data

In this experiment, we adopt the same data generation strategy as in Section 4.1.2, with some minor adjustments. We set $s = 0.1$ and randomly generate a true γ with a non-sparsity level of 0.01, where all non-zero entries are ones. We conduct experiments on synthetic data across various problem dimensions and sample sizes. Additionally, we explore different values of (ρ, λ) , including pairs capable of recovering the true rank of B and the true sparsity level of γ . The results are shown in Tables 5 and 6. Additionally, we plot Figures 2 and 3, corresponding to the parameters with an asterisk from Tables 5 and 6.

Table 5: Time comparison of PPDNA, ADMM, and Nesterov algorithm with penalty parameters in (20) on synthetic data. Here \hat{r} represents the rank of the estimated matrix coefficient B^* by PPDNA, and R_{obj} is given by (19). “P” stands for PPDNA; “A” for ADMM; “N” for Nesterov algorithm. The penalty parameters marked with asterisks (*) are used for plotting Figure 2, as they have been found to recover the true rank of B .

Data	ρ	\hat{r}	Iterations			R_{obj}			Time		
			P	A	N	P	A	N	P	A	N
$n = 500$	1.04e+1	6	13	925	43797	3.01e-16	9.89e-11	4.76e-02	0:01:02	0:02:32	1:00:00
	1.04e+2	6	10	16199	38902	3.23e-11	9.02e-11	3.71e-03	0:00:42	0:34:39	1:00:00
	1.04e+3	6	7	19362	42416	4.36e-12	3.94e-05	7.71e-08	0:00:49	1:00:00	1:00:00
	$q = 200$	6	7	17783	11269	3.35e-14	2.82e-01	9.99e-11	0:01:28	1:00:00	0:13:27
	$p = 300$	5	7	17354	7084	2.30e-13	1.48e-01	9.98e-11	0:01:15	1:00:00	0:09:47
	$r = 5$	4	7	11228	4739	8.92e-14	7.71e-02	1.00e-11	0:01:56	1:00:00	0:07:29
	2.07e+4	4	7	14803	3031	1.33e-14	4.65e-02	9.99e-11	0:02:00	1:00:00	0:04:46
$n = 300$	1.03e+1	6	12	1059	30816	5.97e-11	9.94e-11	9.98e-02	0:01:15	0:04:13	1:00:00
	1.03e+2	6	10	18093	29772	2.85e-11	1.43e-08	1.79e-02	0:01:26	1:00:00	1:00:00
	1.03e+3	6	7	12541	34291	1.93e-11	1.19e+00	8.16e-05	0:01:04	1:00:00	1:00:00
	$n = 300$	6	7	11643	38344	6.42e-14	2.62e-01	3.40e-10	0:02:09	1:00:00	1:00:00
	$p = 300$	5	7	11784	16496	3.65e-14	2.24e-01	1.00e-10	0:01:53	1:00:00	0:28:22
	$r = 5$	5	7	10851	7818	4.38e-13	6.72e-01	9.99e-11	0:01:53	1:00:00	0:12:20
	3.10e+4	3	7	10700	2494	3.87e-13	1.44e-01	9.96e-11	0:01:46	1:00:00	0:04:00
$n = 1000$	1.51e+1	11	12	1019	15443	7.76e-13	9.76e-11	1.42e-01	0:02:08	0:08:24	1:00:00
	1.51e+2	11	8	5010	13846	2.54e-11	9.95e-11	3.20e-02	0:02:19	0:59:10	1:00:00
	1.51e+3	11	7	4137	12688	1.14e-12	7.21e-01	8.13e-04	0:04:42	1:00:00	1:00:00
	$q = 300$	10	7	4098	10236	2.54e-14	4.13e-01	1.00e-11	0:08:01	1:00:00	0:48:14
	$p = 400$	10	7	2854	12481	3.26e-14	2.86e+00	1.87e-10	0:13:07	1:00:00	1:00:00
	$r = 10$	10	7	3973	7698	1.89e-14	1.50e+00	9.98e-11	0:06:59	1:00:00	0:31:38
	3.20e+4	9	7	4044	5536	1.43e-14	9.93e-01	9.99e-11	0:07:42	1:00:00	0:21:39
$n = 400$	1.00e+1	11	13	812	8724	1.18e-12	9.68e-11	3.10e-01	0:05:35	0:13:51	1:00:00
	1.00e+2	11	9	4404	12216	8.81e-11	1.42e-07	7.98e-02	0:03:24	1:00:00	1:00:00
	1.00e+3	11	7	3411	12134	2.09e-12	1.51e+00	9.75e-03	0:04:44	1:00:00	1:00:00
	$q = 400$	10	7	3240	11594	6.29e-14	5.67e+00	2.02e-05	0:10:18	1:00:00	1:00:00
	$p = 400$	9	7	2276	12704	4.03e-14	3.30e+00	3.68e-07	0:13:32	1:00:00	1:00:00
	$r = 10$	9	7	3246	12724	2.64e-14	1.96e+00	7.82e-09	0:10:22	1:00:00	1:00:00
	3.00e+4	9	7	3189	12367	2.08e-14	1.43e+00	6.32e-10	0:10:38	1:00:00	1:00:00

It is clear from Figures 2 and 3 that the convergence speed of the PPDNA significantly surpass that of both Nesterov algorithm and ADMM. Figure 2 reveals that Nesterov algorithm initially descends rapidly. This rapid descent, however, gradually tapers off, which still remains faster than ADMM. Tables 5 and 6 confirm that PPDNA consistently outperforms ADMM and

Nesterov algorithm, achieving rapid convergence to the desired accuracy within several minutes for both regularization settings. ADMM and Nesterov algorithm, in contrast, consistently take much longer time to converge, and sometimes failed to converge to the desired accuracy within an hour. Note that Nesterov algorithm is more efficient when the penalty parameters are larger, indicating its dependence on the regularization parameters for faster convergence. Overall, the PPDNA demonstrates superior efficiency and robustness in various settings.

Table 6: Time comparison of PPDNA and ADMM with penalty parameters in (21) on synthetic data. Here \hat{r} represents the rank of the estimated matrix coefficient B^* by PPDNA, and $\text{ns}(\gamma^*)$ represents the non-sparsity level of the estimated vector coefficient γ^* by PPDNA. The penalty parameters marked with asterisks (*) are used for plotting Figure 3, as they have been found to recover the true rank of B and the true sparsity level of γ .

Data	(ρ, λ)	\hat{r}	$\text{ns}(\gamma^*)$	Iterations		R_{obj}		Time	
				P	A	P	A	P	A
$n = 500$ $m = 300$ $q = 200$ $p = 300$ $r = 5$	(3.46e+1, 2.66e+0)	11	1.00e-2	8	296	5.53e-11	9.57e-11	0:00:12	0:00:52
	(3.46e+2, 2.66e+1)	11	1.00e-2	7	1042	5.75e-12	9.76e-11	0:00:21	0:03:50
	(3.46e+3, 2.66e+2)	11	1.00e-2	7	2724	4.10e-14	9.96e-11	0:00:43	0:08:45
	(2.07e+4, 1.51e+3)	7	1.33e-2	6	3314	5.63e-11	9.76e-11	0:00:26	0:11:58
	(2.42e+4, 1.51e+3)	6	5.00e-2	6	3341	4.06e-11	9.49e-11	0:00:35	0:12:04
	(2.77e+4, 2.41e+3)	6	3.33e-3	6	3365	2.84e-11	9.92e-11	0:00:35	0:19:30
	(3.11e+4, 2.41e+3)	6	6.67e-3	6	3404	1.97e-11	9.19e-11	0:00:35	0:19:21
	(3.46e+4, 2.66e+3)*	5	1.00e-2	6	3424	1.31e-11	9.69e-11	0:00:27	0:13:04
$n = 500$ $m = 300$ $q = 300$ $p = 300$ $r = 5$	(5.17e+1, 3.69e+0)	11	2.00e-2	8	366	3.36e-11	9.50e-11	0:00:20	0:01:27
	(5.17e+2, 3.69e+1)	11	2.00e-2	7	1234	3.13e-12	9.97e-11	0:00:31	0:06:29
	(5.17e+3, 3.69e+2)	11	2.00e-2	7	2903	4.17e-14	9.74e-11	0:01:02	0:14:16
	(3.82e+4, 3.10e+3)	7	3.33e-3	6	3506	3.61e-11	9.08e-11	0:00:44	0:19:59
	(4.13e+4, 3.40e+3)	7	3.33e-3	6	3547	2.95e-11	9.57e-11	0:00:45	0:20:23
	(4.44e+4, 3.71e+3)	6	3.33e-3	6	3578	2.38e-11	9.53e-11	0:00:52	0:25:27
	(4.65e+4, 3.71e+3)	6	3.33e-3	6	3596	2.06e-11	9.82e-11	0:00:50	0:20:41
	(5.17e+4, 3.69e+3)*	5	1.00e-2	6	3647	1.40e-11	9.58e-11	0:00:38	0:20:28
$n = 1000$ $m = 400$ $q = 300$ $p = 400$ $r = 10$	(6.59e+1, 4.98e+0)	15	1.50e-2	8	349	1.39e-11	8.91e-11	0:00:58	0:03:42
	(6.59e+2, 4.98e+1)	15	1.50e-2	7	1265	2.10e-12	9.73e-11	0:01:13	0:13:59
	(6.59e+3, 4.98e+2)	15	1.50e-2	7	2925	5.88e-14	9.73e-11	0:04:51	0:41:28
	(4.70e+4, 3.32e+3)	12	2.00e-2	6	3497	7.51e-11	9.90e-11	0:04:22	0:54:47
	(5.65e+4, 3.32e+3)	11	3.00e-2	6	2538	5.22e-11	5.35e-02	0:06:00	1:00:00
	(6.59e+4, 3.87e+3)	10	3.25e-2	6	3605	3.65e-11	8.98e-11	0:04:12	0:56:43
	(6.59e+4, 4.98e+3)*	10	1.00e-2	6	3607	3.63e-11	9.43e-11	0:04:23	0:58:24
	(7.53e+4, 4.42e+3)	9	3.25e-2	6	3682	2.52e-11	9.79e-11	0:04:05	0:59:57
$n = 1000$ $m = 400$ $q = 400$ $p = 400$ $r = 10$	(9.00e+1, 6.27e+0)	17	1.25e-2	8	425	8.40e-12	9.79e-11	0:01:52	0:09:43
	(9.00e+2, 6.27e+1)	17	1.25e-2	7	1483	1.26e-12	9.90e-11	0:02:26	0:27:24
	(9.00e+3, 6.27e+2)	15	1.25e-2	7	3066	5.49e-14	9.82e-11	0:06:05	0:58:29
	(7.00e+4, 4.67e+3)	12	1.50e-2	6	2845	5.38e-11	1.87e-02	0:05:33	1:00:00
	(9.00e+4, 6.01e+3)	10	1.50e-2	6	2019	2.90e-11	2.76e-01	0:06:58	1:00:00
	(9.00e+4, 6.27e+3)*	10	1.00e-2	6	2517	2.90e-11	2.75e-01	0:04:51	1:00:00
	(1.00e+5, 5.34e+3)	9	4.75e-2	6	2425	2.12e-11	2.01e-01	0:07:53	1:00:00
	(1.20e+5, 5.34e+3)	7	9.25e-2	6	2845	1.08e-11	8.81e-02	0:05:04	1:00:00

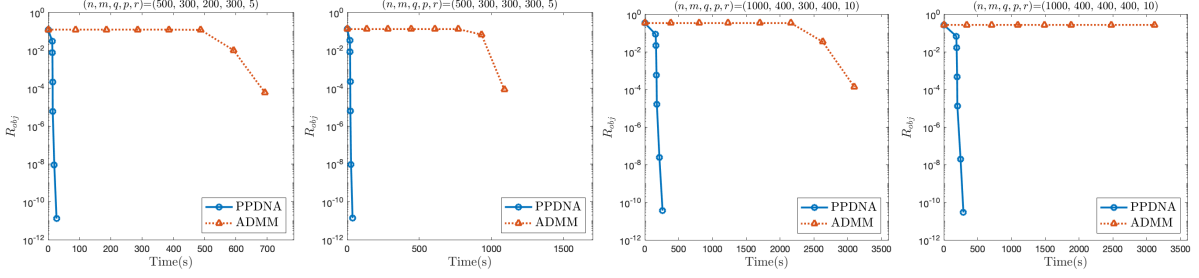


Figure 3: Time vs. R_{obj} (see (19)) of PPDNA and ADMM on synthetic data. The penalty parameters are taken from Table 6 with asterisks (*).

4.2.2 COVID-19 Data

In this subsection, we conduct numerical experiments on the COVID-19 data [52], which can be downloaded from <https://health.google.com/covid-19/open-data/>. This data offers a comprehensive daily time-series of COVID-19 cases, deaths, recoveries, tests, vaccinations, and hospitalizations across more than 230 countries, 760 regions, and 12,000 lower-level administrative divisions. In our analysis, we concentrate on 181 regions over a period of 911 days from January 1, 2020, to June 30, 2022.

The response variable y represents the total count of confirmed cases within each region during this period. Each matrix-valued data X_i , for all $i \in [181]$ encompasses various COVID-19 related information, each of which fluctuates over the 911-day period, including:

1. Government response implemented daily, which contains 20 factors such as school closures, gathering restrictions, stay-at-home mandates, and income support initiatives.
2. Mobility, which contains 6 factors reflecting different aspects of people's movement patterns, such as percentage changes in visits to restaurants, cafes, shopping centers, theme parks, museums, libraries, and movie theaters compared to the baseline.
3. Weather, which contains 7 weather related factors including recorded hourly average, minimum and maximum temperature, rainfall and snowfall during the entire day.
4. Vaccination trends, which contains 30 factors related to deployment and administration of COVID-19 vaccines, such as the count of new persons which have received one or more doses.

Therefore, each X_i is of size 911×63 , resulting from 911-day framework and a total of 63 measurements derived from the aforementioned information. Additionally, the vector-valued sample $z_i \in \mathbb{R}^{13}$ encapsulates 13 health-related characteristics for each region that remain relatively constant or exhibit minimal variation during the 911-day period. These characteristics include factors such as life expectancy, hospital bed capacity, prevalence of diabetes and smoking, and the number of nurses. During the data pre-processing, we replaced the missing values by 0. In addition, we standardized both the matrices X_i 's and the matrix Z column-wisely. The response variable y is also standardized. For clarity, we specify the dimensions as follows: $m = 911$, $q = 63$, $p = 13$, and $n = 181$.

Table 7 compares PPDNA and ADMM on COVID-19 data across a wide range of α_1 and α_2 values in (21), resulting in various values of ρ and λ . Additionally, Table 8 includes Nesterov algorithm alongside PPDNA and ADMM in the comparison, with a broad selection of α values in (20), highlighting the performance without regularization on the vector coefficient.

We can see from Table 7 that PPDNA consistently outperforms ADMM in terms of computational time. PPDNA typically achieves the desired accuracy in less than one minute, whereas ADMM often takes several minutes to converge. Additionally, in Table 8, Nesterov algorithm exhibits even slower convergence and occasionally fails to descend, terminating prematurely.

By combining the findings presented in Section 4.2, we can safely conclude that PPDNA

emerges as a significantly more efficient and robust algorithm compared to ADMM and Nesterov algorithm, for estimating both matrix and vector variables in problem (3).

Table 7: Time comparison of PPDNA and ADMM with penalty parameters in (21) on COVID-19 data. Here \hat{r} represents the rank of the estimated matrix coefficient B^* by PPDNA, $\text{ns}(\gamma^*)$ represents the non-sparsity level of the estimated vector coefficient γ^* by PPDNA, and R_{obj} is given by (19).

α_1	α_2	\hat{r}	$\text{ns}(\gamma^*)$	Iterations		R_{obj}		Time	
				P	A	P	A	P	A
1e-1	1e-1	3	7.69e-2	10	2747	1.74e-11	9.80e-11	0:00:16	0:07:51
	5e-2	3	4.62e-1	9	2715	4.89e-11	9.73e-11	0:00:17	0:07:44
	1e-2	3	9.23e-1	9	2779	9.91e-11	9.84e-11	0:00:18	0:07:50
1e-2	1e-2	4	1.54e-1	11	1016	9.69e-11	9.73e-11	0:00:15	0:02:34
	5e-3	4	6.15e-1	12	962	3.11e-12	9.91e-11	0:00:16	0:02:27
	1e-3	4	8.46e-1	13	1227	8.80e-12	9.89e-11	0:00:19	0:03:08
1e-3	1e-3	5	1.54e-1	11	311	2.14e-12	9.14e-11	0:00:16	0:00:47
	5e-4	4	6.92e-1	13	544	3.82e-12	9.93e-11	0:00:24	0:01:29
	1e-4	4	8.46e-1	17	1615	2.36e-11	9.92e-11	0:00:19	0:03:01
1e-4	1e-4	5	1.54e-1	19	447	8.51e-12	9.87e-11	0:00:11	0:00:45
	5e-5	4	6.92e-1	36	2111	8.55e-11	9.98e-11	0:00:17	0:03:41
	1e-5	4	8.46e-1	18	4830	5.51e-11	9.98e-11	0:00:22	0:07:40
1e-5	1e-5	5	1.54e-1	42	2441	9.57e-11	9.96e-11	0:00:16	0:03:35
	5e-6	4	6.92e-1	100	6460	0.00e+00	9.99e-11	0:00:31	0:09:20
	1e-6	4	8.46e-1	100	9903	0.00e+00	9.54e-11	0:00:38	0:14:22

Table 8: Time comparison of PPDNA, ADMM, and Nesterov algorithm with penalty parameters in (20) on COVID-19 data. Here \hat{r} represents the rank of the estimated matrix coefficient B^* by PPDNA, and R_{obj} is given by (19).

α	\hat{r}	Iterations			R_{obj}			Time		
		P	A	N	P	A	N	P	A	N
1e-1	3	10	3188	20080	1.30e-11	9.90e-11	1.00e-10	0:00:18	0:09:32	0:05:14
1e-2	4	12	1783	228555	2.19e-11	9.95e-11	6.97e-07	0:00:24	0:04:33	1:00:00
1e-3	4	15	1750	218431	5.95e-11	9.95e-11	5.27e-03	0:00:28	0:03:21	1:00:00
1e-4	4	27	5981	229822	9.46e-11	9.99e-11	1.06e-02	0:00:26	0:09:21	1:00:00
1e-5	4	97	14030	2991	6.07e-11	9.79e-11	4.30e-03	0:00:45	0:19:17	0:00:51

5 Conclusion and Discussion

In this paper, we proposed a class of regularized regression models that can incorporate the matrix and vector predictors simultaneously with general convex penalty functions. The n -consistency and \sqrt{n} -consistency of the estimator obtained from the optimization model were established when nuclear norm and lasso norm penalties are employed. We proposed a highly efficient dual semismooth Newton method based preconditioned proximal point algorithm for solving the general model, which fully exploits the second-order information. Extensive numerical experiments were conducted to demonstrate the practical and general applicability of our

proposed algorithm, as well as its efficiency and robustness compared to the state-of-the-art algorithms for solving regularized regression models. While this paper primarily focuses on linear regression problems, our algorithm can handle other problems, including logistic regression and Poisson regression problems. Expanding our consistency analysis for other loss and penalty functions remains an open question, as we currently address a special case in Section 2. Additionally, when dealing with possibly non-convex loss and penalty functions, we may need to combine our algorithmic framework with difference-of-convex (d.c.) tools and majorization techniques to design d.c. type algorithms.

A Proof of Theorem 2.1

Proof of Theorem 2.1 For any given $(U, \beta) \in \mathbb{R}^{m \times q} \times \mathbb{R}^p$, we have that

$$\begin{aligned}
& Z_n(U, \beta) - Z(U, \beta) \\
&= \frac{1}{n} \sum_{i=1}^n (y_i - \langle X_i, U \rangle - \langle z_i, \beta \rangle)^2 + \frac{\rho_n}{n} \|U\|_* + \frac{\lambda_n}{n} \|\beta\|_1 - \text{vec}(U - B)^\top C \text{vec}(U - B) \\
&\quad - 2 \text{vec}(U - B)^\top H(\beta - \gamma) - (\beta - \gamma)^\top D(\beta - \gamma) - \rho_0 \|U\|_* - \lambda_0 \|\beta\|_1 \\
&= \frac{1}{n} \sum_{i=1}^n (\varepsilon_i - \langle X_i, U - B \rangle - \langle z_i, \beta - \gamma \rangle)^2 - \text{vec}(U - B)^\top C \text{vec}(U - B) \\
&\quad - 2 \text{vec}(U - B)^\top H(\beta - \gamma) - (\beta - \gamma)^\top D(\beta - \gamma) + \left(\frac{\rho_n}{n} - \rho_0 \right) \|U\|_* + \left(\frac{\lambda_n}{n} - \lambda_0 \right) \|\beta\|_1 \\
&= \frac{1}{n} \sum_{i=1}^n \varepsilon_i^2 + \frac{1}{n} \sum_{i=1}^n (\langle X_i, U - B \rangle)^2 + \frac{1}{n} \sum_{i=1}^n (\langle z_i, \beta - \gamma \rangle)^2 - \frac{2}{n} \sum_{i=1}^n \varepsilon_i \langle X_i, U - B \rangle \\
&\quad - \frac{2}{n} \sum_{i=1}^n \varepsilon_i \langle z_i, \beta - \gamma \rangle + \frac{2}{n} \sum_{i=1}^n \langle X_i, U - B \rangle \langle z_i, \beta - \gamma \rangle - \text{vec}(U - B)^\top C \text{vec}(U - B) \\
&\quad - 2 \text{vec}(U - B)^\top H(\beta - \gamma) - (\beta - \gamma)^\top D(\beta - \gamma) + \left(\frac{\rho_n}{n} - \rho_0 \right) \|U\|_* + \left(\frac{\lambda_n}{n} - \lambda_0 \right) \|\beta\|_1 \\
&= \frac{1}{n} \sum_{i=1}^n \varepsilon_i^2 + \text{vec}(U - B)^\top (C_n - C) \text{vec}(U - B) + (\beta - \gamma)^\top (D_n - D) (\beta - \gamma) \\
&\quad + 2 \text{vec}(U - B)^\top (H_n - H) (\beta - \gamma) - \frac{2}{n} \sum_{i=1}^n \varepsilon_i (\langle X_i, U - B \rangle + \langle z_i, \beta - \gamma \rangle) \\
&\quad + \left(\frac{\rho_n}{n} - \rho_0 \right) \|U\|_* + \left(\frac{\lambda_n}{n} - \lambda_0 \right) \|\beta\|_1.
\end{aligned}$$

By the weak law of large numbers, we have that $\frac{1}{n} \sum_{i=1}^n \varepsilon_i^2 \rightarrow \mathbb{E}[\varepsilon_i^2] = \sigma^2$ in probability as $n \rightarrow \infty$.

Moreover, it can be seen that

$$\begin{aligned}
& \mathbb{E} \left[\frac{1}{n} \sum_{i=1}^n \varepsilon_i (\langle X_i, U - B \rangle + \langle z_i, \beta - \gamma \rangle) \right] = \frac{1}{n} \sum_{i=1}^n \mathbb{E}[\varepsilon_i] (\langle X_i, U - B \rangle + \langle z_i, \beta - \gamma \rangle) = 0, \\
& \text{Var} \left[\frac{1}{n} \sum_{i=1}^n \varepsilon_i (\langle X_i, U - B \rangle + \langle z_i, \beta - \gamma \rangle) \right] = \mathbb{E} \left[\frac{1}{n^2} \sum_{i=1}^n \varepsilon_i^2 (\langle X_i, U - B \rangle + \langle z_i, \beta - \gamma \rangle)^2 \right] \\
&= \frac{1}{n^2} \sum_{i=1}^n \mathbb{E}[\varepsilon_i^2] (\langle X_i, U - B \rangle + \langle z_i, \beta - \gamma \rangle)^2 = \frac{\sigma^2}{n} \begin{pmatrix} \text{vec}(U - B) \\ \beta - \gamma \end{pmatrix}^\top S_n \begin{pmatrix} \text{vec}(U - B) \\ \beta - \gamma \end{pmatrix} := \frac{\sigma^2}{n} \hat{\sigma}_n^2.
\end{aligned}$$

Here, $\hat{\sigma}_n^2 > 0$ for large n because $\hat{\sigma}_n^2$ converges to a positive number, as long as $(U, \beta) \neq (B, \gamma)$. In cases where they are equal, $\frac{1}{n} \sum_{i=1}^n \varepsilon_i (\langle X_i, U-B \rangle + \langle z_i, \beta-\gamma \rangle)$ is zero. By Chebyshev's inequality, for any given $\epsilon > 0$, we have that

$$\mathbb{P} \left(\left| \frac{1}{n} \sum_{i=1}^n \varepsilon_i (\langle X_i, U-B \rangle + \langle z_i, \beta-\gamma \rangle) \right| \geq \epsilon \right) \leq \frac{\sigma^2 \hat{\sigma}_n^2}{\epsilon^2 n},$$

which further implies that $\lim_{n \rightarrow \infty} \mathbb{P} \left(\left| \frac{1}{n} \sum_{i=1}^n \varepsilon_i (\langle X_i, U-B \rangle + \langle z_i, \beta-\gamma \rangle) \right| \geq \epsilon \right) = 0$. Therefore, we have proved that $Z_n(U, \beta) - Z(U, \beta) \rightarrow \sigma^2$ in probability as $n \rightarrow \infty$. According to Pollard [42], we further have

$$\sup_{(U, \beta) \in K} \left| Z_n(U, \beta) - Z(U, \beta) - \sigma^2 \right| \rightarrow 0 \quad (22)$$

in probability as $n \rightarrow \infty$, for any compact set $K \subset \mathbb{R}^{m \times q} \times \mathbb{R}^p$.

Next, we denote $Z_n^{(0)}(U, \beta) := \frac{1}{n} \sum_{i=1}^n (y_i - \langle X_i, U \rangle - \langle z_i, \beta \rangle)^2$, and assume that it is minimized at $(\hat{B}_n^{(0)}, \hat{\gamma}_n^{(0)})$.

Then we have

$$\begin{aligned} \frac{1}{n} \sum_{i=1}^n \left(y_i - \langle X_i, \hat{B}_n^{(0)} \rangle - \langle z_i, \hat{\gamma}_n^{(0)} \rangle \right)^2 &\leq \frac{1}{n} \sum_{i=1}^n (y_i - \langle X_i, B \rangle - \langle z_i, \gamma \rangle)^2, \\ \frac{1}{n} \sum_{i=1}^n \left(\varepsilon_i - \langle X_i, \hat{B}_n^{(0)} - B \rangle - \langle z_i, \hat{\gamma}_n^{(0)} - \gamma \rangle \right)^2 &\leq \frac{1}{n} \sum_{i=1}^n \varepsilon_i^2. \end{aligned}$$

Then we can see that

$$\begin{aligned} &\begin{pmatrix} \text{vec}(\hat{B}_n^{(0)} - B) \\ \hat{\gamma}_n^{(0)} - \gamma \end{pmatrix}^\top S_n \begin{pmatrix} \text{vec}(\hat{B}_n^{(0)} - B) \\ \hat{\gamma}_n^{(0)} - \gamma \end{pmatrix} \\ &= \text{vec}(\hat{B}_n^{(0)} - B)^\top C_n \text{vec}(\hat{B}_n^{(0)} - B) + (\hat{\gamma}_n^{(0)} - \gamma)^\top D_n (\hat{\gamma}_n^{(0)} - \gamma) + 2 \text{vec}(\hat{B}_n^{(0)} - B)^\top H_n (\hat{\gamma}_n^{(0)} - \gamma) \\ &= \frac{1}{n} \sum_{i=1}^n \left(\langle X_i, \hat{B}_n^{(0)} - B \rangle + \langle z_i, \hat{\gamma}_n^{(0)} - \gamma \rangle \right)^2 = \frac{1}{n} \sum_{i=1}^n \left(\langle X_i, \hat{B}_n^{(0)} - B \rangle + \langle z_i, \hat{\gamma}_n^{(0)} - \gamma \rangle - \varepsilon_i + \varepsilon_i \right)^2 \\ &\leq \frac{2}{n} \sum_{i=1}^n \left(\langle X_i, \hat{B}_n^{(0)} - B \rangle + \langle z_i, \hat{\gamma}_n^{(0)} - \gamma \rangle - \varepsilon_i \right)^2 + \frac{2}{n} \sum_{i=1}^n \varepsilon_i^2 \leq \frac{4}{n} \sum_{i=1}^n \varepsilon_i^2. \end{aligned}$$

By Assumption 1 and the positive definiteness of S , there exists $\eta > 0$ such that $S_n \succeq \eta I_{mq+p}$ for large n . Therefore,

$$\eta \left(\|\hat{B}_n^{(0)} - B\|_F^2 + \|\hat{\gamma}_n^{(0)} - \gamma\|^2 \right) \leq \frac{4}{n} \sum_{i=1}^n \varepsilon_i^2. \quad (23)$$

Since $\sum_{i=1}^n (\varepsilon_i / \sigma)^2$ follows the chi-squared distribution with n degrees of freedom, we have $\mathbb{E} \left[\frac{1}{n} \sum_{i=1}^n \varepsilon_i^2 \right] = \sigma^2$ and $\text{Var} \left[\frac{1}{n} \sum_{i=1}^n \varepsilon_i^2 \right] = \frac{2\sigma^4}{n}$. Then from (23) and Chebyshev's inequality,

$$\begin{aligned} \mathbb{P} \left(\|\hat{B}_n^{(0)} - B\|_F^2 + \|\hat{\gamma}_n^{(0)} - \gamma\|^2 > \frac{4}{\eta} (\sigma^2 + 1) \right) &\leq \mathbb{P} \left(\frac{1}{n} \sum_{i=1}^n \varepsilon_i^2 > \sigma^2 + 1 \right) \\ &\leq \mathbb{P} \left(\left| \frac{1}{n} \sum_{i=1}^n \varepsilon_i^2 - \sigma^2 \right| \geq 1 \right) \leq \frac{2\sigma^4}{n}, \end{aligned}$$

which further implies that

$$\lim_{n \rightarrow \infty} \mathbb{P} \left(\|\hat{B}_n^{(0)} - B\|_F^2 + \|\hat{\gamma}_n^{(0)} - \gamma\|^2 > \frac{4}{\eta} (\sigma^2 + 1) \right) = 0. \quad (24)$$

This means that $\{(\hat{B}_n^{(0)}, \hat{\gamma}_n^{(0)})\}$ is bounded in probability, i.e., $(\hat{B}_n^{(0)}, \hat{\gamma}_n^{(0)}) = O_P(1)$. Furthermore, due to the fact that $Z_n(\hat{B}_n, \hat{\gamma}_n) \leq Z_n(\hat{B}_n^{(0)}, \hat{\gamma}_n^{(0)})$ and $Z_n^{(0)}(\hat{B}_n^{(0)}, \hat{\gamma}_n^{(0)}) \leq Z_n^{(0)}(\hat{B}_n, \hat{\gamma}_n)$, we have

$$\begin{aligned} & \frac{1}{n} \sum_{i=1}^n \left(y_i - \langle X_i, \hat{B}_n \rangle - \langle z_i, \hat{\gamma}_n \rangle \right)^2 + \frac{\rho_n}{n} \|\hat{B}_n\|_* + \frac{\lambda_n}{n} \|\hat{\gamma}_n\|_1 \\ & \leq \frac{1}{n} \sum_{i=1}^n \left(y_i - \langle X_i, \hat{B}_n^{(0)} \rangle - \langle z_i, \hat{\gamma}_n^{(0)} \rangle \right)^2 + \frac{\rho_n}{n} \|\hat{B}_n^{(0)}\|_* + \frac{\lambda_n}{n} \|\hat{\gamma}_n^{(0)}\|_1 \\ & \leq \frac{1}{n} \sum_{i=1}^n \left(y_i - \langle X_i, \hat{B}_n \rangle - \langle z_i, \hat{\gamma}_n \rangle \right)^2 + \frac{\rho_n}{n} \|\hat{B}_n^{(0)}\|_* + \frac{\lambda_n}{n} \|\hat{\gamma}_n^{(0)}\|_1, \end{aligned}$$

which means

$$\frac{\rho_n}{n} \|\hat{B}_n\|_* + \frac{\lambda_n}{n} \|\hat{\gamma}_n\|_1 \leq \frac{\rho_n}{n} \|\hat{B}_n^{(0)}\|_* + \frac{\lambda_n}{n} \|\hat{\gamma}_n^{(0)}\|_1. \quad (25)$$

Therefore, the sequence $\{(\hat{B}_n, \hat{\gamma}_n)\}$ is also bounded in probability: $(\hat{B}_n, \hat{\gamma}_n) = O_P(1)$.

Lastly, for any compact set $K \subset \mathbb{R}^{m \times q} \times \mathbb{R}^p$, we have

$$\sup_{(U, \beta) \in K} \left| Z_n(U, \beta) - Z(U, \beta) - \sigma^2 \right| \geq \left| \inf_{(U, \beta) \in K} Z_n(U, \beta) - \inf_{(U, \beta) \in K} Z(U, \beta) - \sigma^2 \right|,$$

due to the following two inequalities:

$$\begin{aligned} & \inf_{(U, \beta) \in K} Z_n(U, \beta) - \inf_{(U, \beta) \in K} Z(U, \beta) - \sigma^2 = - \sup_{(U, \beta) \in K} (-Z_n(U, \beta)) + \sup_{(U, \beta) \in K} (-Z(U, \beta) - \sigma^2) \\ & \leq \sup_{(U, \beta) \in K} (Z_n(U, \beta) - Z(U, \beta) - \sigma^2) \leq \sup_{(U, \beta) \in K} \left| Z_n(U, \beta) - Z(U, \beta) - \sigma^2 \right|, \\ & - \inf_{(U, \beta) \in K} Z_n(U, \beta) + \inf_{(U, \beta) \in K} Z(U, \beta) + \sigma^2 = \sup_{(U, \beta) \in K} (-Z_n(U, \beta)) - \sup_{(U, \beta) \in K} (-Z(U, \beta) - \sigma^2) \\ & \leq \sup_{(U, \beta) \in K} (-Z_n(U, \beta) + Z(U, \beta) + \sigma^2) \leq \sup_{(U, \beta) \in K} \left| Z_n(U, \beta) - Z(U, \beta) - \sigma^2 \right|. \end{aligned}$$

By (24) and (25), there exists $M > 0$ such that

$$\lim_{n \rightarrow \infty} \mathbb{P} \left(\|\hat{B}_n\|^2 + \|\hat{\gamma}_n\|^2 > M \right) = 0. \quad (26)$$

Denote $K_n := \{(\hat{B}_n, \hat{\gamma}_n), (\hat{B}, \hat{\gamma})\}$ and $K_0 := \{(B, \gamma) \in \mathbb{R}^{m \times q} \times \mathbb{R}^p \mid \|B\|^2 + \|\gamma\|^2 \leq M\} \cup \{(\hat{B}, \hat{\gamma})\}$. Then we have that

$$\begin{aligned} & |Z(\hat{B}_n, \hat{\gamma}_n) - Z(\hat{B}, \hat{\gamma})| \leq |Z_n(\hat{B}_n, \hat{\gamma}_n) - Z(\hat{B}_n, \hat{\gamma}_n) - \sigma^2| + |Z_n(\hat{B}_n, \hat{\gamma}_n) - Z(\hat{B}, \hat{\gamma}) - \sigma^2| \\ & \leq \sup_{(U, \beta) \in K_n} |Z_n(U, \beta) - Z(U, \beta) - \sigma^2| + \left| \inf_{(U, \beta) \in K_n} Z_n(U, \beta) - \inf_{(U, \beta) \in K_n} Z(U, \beta) - \sigma^2 \right| \\ & \leq 2 \sup_{(U, \beta) \in K_n} |Z_n(U, \beta) - Z(U, \beta) - \sigma^2|. \end{aligned}$$

Therefore, for any $\epsilon > 0$, we can see that

$$\begin{aligned} & \mathbb{P} \left(|Z(\hat{B}_n, \hat{\gamma}_n) - Z(\hat{B}, \hat{\gamma})| \geq \epsilon \right) \\ & = \mathbb{P} \left(|Z(\hat{B}_n, \hat{\gamma}_n) - Z(\hat{B}, \hat{\gamma})| \geq \epsilon, \|\hat{B}_n\|^2 + \|\hat{\gamma}_n\|^2 \leq M \right) \\ & \quad + \mathbb{P} \left(|Z(\hat{B}_n, \hat{\gamma}_n) - Z(\hat{B}, \hat{\gamma})| \geq \epsilon, \|\hat{B}_n\|^2 + \|\hat{\gamma}_n\|^2 > M \right) \\ & \leq \mathbb{P} \left(\|\hat{B}_n\|^2 + \|\hat{\gamma}_n\|^2 \leq M \right) \mathbb{P} \left(|Z(\hat{B}_n, \hat{\gamma}_n) - Z(\hat{B}, \hat{\gamma})| \geq \epsilon \mid \|\hat{B}_n\|^2 + \|\hat{\gamma}_n\|^2 \leq M \right) \end{aligned}$$

$$\begin{aligned}
& + \mathbb{P} \left(\|\widehat{B}_n\|^2 + \|\widehat{\gamma}_n\|^2 > M \right) \\
& \leq \mathbb{P} \left(\|\widehat{B}_n\|^2 + \|\widehat{\gamma}_n\|^2 \leq M \right) \mathbb{P} \left(\sup_{(U, \beta) \in K_n} |Z_n(U, \beta) - Z(U, \beta) - \sigma^2| \geq \frac{\epsilon}{2} \middle| \|\widehat{B}_n\|^2 + \|\widehat{\gamma}_n\|^2 \leq M \right) \\
& \quad + \mathbb{P} \left(\|\widehat{B}_n\|^2 + \|\widehat{\gamma}_n\|^2 > M \right) \\
& \leq \mathbb{P} \left(\|\widehat{B}_n\|^2 + \|\widehat{\gamma}_n\|^2 \leq M \right) \mathbb{P} \left(\sup_{(U, \beta) \in K_0} |Z_n(U, \beta) - Z(U, \beta) - \sigma^2| \geq \frac{\epsilon}{2} \middle| \|\widehat{B}_n\|^2 + \|\widehat{\gamma}_n\|^2 \leq M \right) \\
& \quad + \mathbb{P} \left(\|\widehat{B}_n\|^2 + \|\widehat{\gamma}_n\|^2 > M \right), \\
& = \mathbb{P} \left(\sup_{(U, \beta) \in K_0} |Z_n(U, \beta) - Z(U, \beta) - \sigma^2| \geq \epsilon/2 \right) + \mathbb{P} \left(\|\widehat{B}_n\|^2 + \|\widehat{\gamma}_n\|^2 > M \right),
\end{aligned}$$

where the last inequality holds since $K_n \subset K_0$ given that $\|\widehat{B}_n\|^2 + \|\widehat{\gamma}_n\|^2 \leq M$. Thus, with (22) and (26), we have $\lim_{n \rightarrow \infty} \mathbb{P} \left(|Z(\widehat{B}_n, \widehat{\gamma}_n) - Z(\widehat{B}, \widehat{\gamma})| \geq \epsilon \right) = 0$, which means that $Z(\widehat{B}_n, \widehat{\gamma}_n) \rightarrow Z(\widehat{B}, \widehat{\gamma})$ in probability as $n \rightarrow \infty$. The function $Z(\cdot, \cdot)$ is strongly convex under the assumption that $S \succ 0$, which implies that $(\widehat{B}_n, \widehat{\gamma}_n) \rightarrow (\widehat{B}, \widehat{\gamma})$ in probability as $n \rightarrow \infty$. This completes the proof. \blacksquare

B Preliminaries on Non-smooth Analysis

In this section, we give a brief introduction to some basic concepts and some properties, which is critical for developing the semismooth Newton (SSN) method for solving the subsubproblems (16) in the preconditioned proximal point algorithm (PPA).

Let $\mathcal{F} : \mathbb{R}^n \rightarrow \mathbb{R}^m$ be a locally Lipschitz continuous function. Then by Rademacher's theorem, \mathcal{F} is (Fréchet) differentiable almost everywhere. Let $D_{\mathcal{F}}$ be the set of points in \mathbb{R}^n where \mathcal{F} is differentiable and $\mathcal{F}'(x)$ be the Jacobian of \mathcal{F} at $x \in D_{\mathcal{F}}$. The Bouligand subdifferential (B-subdifferential) of \mathcal{F} at any $x \in \mathbb{R}^n$ is defined as

$$\partial_B \mathcal{F}(x) = \left\{ \lim_{x^k \rightarrow x} \mathcal{F}'(x^k) \mid x^k \in D_{\mathcal{F}} \right\},$$

and the Clarke generalized Jacobian of \mathcal{F} at $x \in \mathbb{R}^n$ is defined as the convex hull of $\partial_B \mathcal{F}(x)$: $\partial \mathcal{F}(x) = \text{conv}\{\partial_B \mathcal{F}(x)\}$. The following definition of “semismoothness with respect to a multifunction”, which is mainly adopted from Qi and Sun [43], Sun and Sun [47], Mifflin [37], Kummer [25], Li et al. [30], is important in the SSN method.

Definition B.1. Let $\mathcal{O} \subseteq \mathbb{R}^n$ be an open set, $\mathcal{K} : \mathcal{O} \rightrightarrows \mathbb{R}^{m \times n}$ be a nonempty, compact valued, upper semicontinuous multifunction, and $\mathcal{F} : \mathcal{O} \rightarrow \mathbb{R}^m$ be a locally Lipschitz continuous function. \mathcal{F} is said to be semismooth at $x \in \mathcal{O}$ with respect to the multifunction \mathcal{K} if \mathcal{F} is directionally differentiable at x and for any $V \in \mathcal{K}(x + \Delta x)$ with $\Delta x \rightarrow 0$,

$$\mathcal{F}(x + \Delta x) - \mathcal{F}(x) - V\Delta x = o(\|\Delta x\|).$$

Let α be a positive constant. \mathcal{F} is said to be α -order (strongly, if $\alpha = 1$) semismooth at $x \in \mathcal{O}$ with respect to \mathcal{K} if \mathcal{F} is directionally differentiable at x and for any $V \in \mathcal{K}(x + \Delta x)$ with $\Delta x \rightarrow 0$,

$$\mathcal{F}(x + \Delta x) - \mathcal{F}(x) - V\Delta x = O(\|\Delta x\|^{1+\alpha}).$$

\mathcal{F} is said to be a semismooth (respectively, α -order semismooth, strongly semismooth) function on \mathcal{O} with respect to \mathcal{K} if it is semismooth (respectively, α -order semismooth, strongly semismooth) everywhere in \mathcal{O} with respect to \mathcal{K} .

C Implementation Details

C.1 ADMM for Solving the Dual Problem

In this subsection, we briefly introduce the well known alternating direction method of multipliers (ADMM) for solving (3). With the auxiliary variable $s \in \mathbb{R}^n$, the primal problem (3) is equivalent to

$$\min_{B \in \mathbb{R}^{m \times q}, \gamma \in \mathbb{R}^p, s \in \mathbb{R}^n} \left\{ h(s) + \phi(B) + \psi(\gamma) \mid X \text{vec}(B) + Z\gamma - s = 0 \right\}. \quad (27)$$

It is not difficult to derive the Lagrangian dual problem of (27), given by

$$\min_{\xi \in \mathbb{R}^n} \left\{ h^*(\xi) + \phi^*(-\text{mat}(X^\top \xi)) + \psi^*(-Z^\top \xi) \right\}.$$

And this dual problem can be further written as

$$\min_{w, \xi \in \mathbb{R}^n, U \in \mathbb{R}^{m \times q}, \beta \in \mathbb{R}^p} \left\{ h^*(w) + \phi^*(U) + q^*(\beta) \mid \text{mat}(X^\top \xi) + U = 0, Z^\top \xi + \beta = 0, w - \xi = 0 \right\}. \quad (28)$$

For $\sigma > 0$, the augmented Lagrangian function associated with the dual problem (28) is

$$\begin{aligned} L_\sigma(w, \xi, U, \beta; B, \gamma, s) &= h^*(w) + \phi^*(U) + \psi^*(\beta) - \langle B, \text{mat}(X^\top \xi) + U \rangle - \langle \gamma, Z^\top \xi + \beta \rangle - \langle s, w - \xi \rangle \\ &\quad + \frac{\sigma}{2} \|\text{mat}(X^\top \xi) + U\|^2 + \frac{\sigma}{2} \|Z^\top \xi + \beta\|^2 + \frac{\sigma}{2} \|w - \xi\|^2 \\ &= h^*(w) + \phi^*(U) + \psi^*(\beta) + \frac{\sigma}{2} \|\text{mat}(X^\top \xi) + U - \frac{1}{\sigma} B\|^2 + \frac{\sigma}{2} \|Z^\top \xi + \beta - \frac{1}{\sigma} \gamma\|^2 \\ &\quad + \frac{\sigma}{2} \|w - \xi - \frac{1}{\sigma} s\|^2 - \frac{1}{2\sigma} \|B\|^2 - \frac{1}{2\sigma} \|\gamma\|^2 - \frac{1}{2\sigma} \|s\|^2. \end{aligned}$$

And the ADMM for solving (28) has the iterations

$$\xi^{k+1} = \arg \min_{\xi} L_\sigma(w^k, \xi, U^k, \beta^k; B^k, \gamma^k, s^k), \quad (29)$$

$$(w^{k+1}, U^{k+1}, \beta^{k+1}) = \arg \min_{w, U, \beta} L_\sigma(w, \xi^{k+1}, U, \beta; B^k, \gamma^k, s^k), \quad (30)$$

$$B^{k+1} = B^k - \tau \sigma (\text{mat}(X^\top \xi^{k+1}) + U^{k+1}),$$

$$\gamma^{k+1} = \gamma^k - \tau \sigma (Z^\top \xi^{k+1} + \beta^{k+1}),$$

$$s^{k+1} = s^k - \tau \sigma (w^{k+1} - \xi^{k+1}),$$

where $\tau \in (0, (1 + \sqrt{5})/2)$ is the step size. Note that the convergence result of ADMM is well documented [18, 15, 17].

By setting the gradient with respect to ξ to be zero, we can deduce that the subproblem (29) is equivalent to solving a linear system $\xi^{k+1} = (I_n + X X^\top + Z Z^\top)^{-1} (X \text{vec}(\frac{1}{\sigma} B^k - U^k) + Z(\frac{1}{\sigma} \gamma^k - \beta^k) + w^k - \frac{1}{\sigma} s^k)$. With the definition of the proximal mapping, problem (30) can be updated as follows:

$$\begin{aligned} w^{k+1} &= \xi^{k+1} + \frac{1}{\sigma} s^k - \frac{1}{\sigma} \text{Prox}_{\sigma h}(\sigma \xi^{k+1} + s^k), \\ U^{k+1} &= \frac{1}{\sigma} B^k - \text{mat}(X^\top \xi^{k+1}) - \frac{1}{\sigma} \text{Prox}_{\sigma \phi}(B^k - \sigma \text{mat}(X^\top \xi^{k+1})), \\ \beta^{k+1} &= \frac{1}{\sigma} \gamma^k - Z^\top \xi^{k+1} - \frac{1}{\sigma} \text{Prox}_{\sigma \psi}(\gamma^k - \sigma Z^\top \xi^{k+1}). \end{aligned}$$

The KKT conditions associated with (27) and (28) are

$$\begin{aligned} X\text{vec}(B) + Z\gamma - s &= 0, \quad \text{mat}(X^\top \xi) + U = 0, \quad Z^\top \xi + \beta = 0, \quad w - \xi = 0, \\ B &= \text{Prox}_\phi(B + U), \quad \gamma = \text{Prox}_\psi(\gamma + \beta), \quad s = \text{Prox}_h(s + w). \end{aligned}$$

Corresponding to the above KKT conditions, we define the KKT residual terms R_p, R_d, R_c :

$$\begin{aligned} R_p &:= \frac{\|X\text{vec}(B) + Z\gamma - s\|}{1 + \|s\|}, \quad R_d := \max \left\{ \frac{\|\text{mat}(X^\top \xi) + U\|_F}{1 + \|U\|_F}, \frac{\|Z^\top \xi + \beta\|}{1 + \|\beta\|}, \frac{\|w - \xi\|}{1 + \|\xi\|} \right\}, \\ R_c &:= \max \left\{ \frac{\|\text{Prox}_\phi(B + U) - B\|_F}{1 + \|B\|_F}, \frac{\|\text{Prox}_\psi(\gamma + \beta) - \gamma\|}{1 + \|\gamma\|}, \frac{\|\text{Prox}_h(s + w) - s\|}{1 + \|s\|} \right\}, \end{aligned} \quad (31)$$

which represent the primal, dual infeasibilities and complementary condition, respectively.

C.2 Discussions on parameter tuning strategies for λ and λ'

Setting $\lambda = \lambda'$ reflects a trade-off between the running time of model selection and prediction accuracy. Using distinct values for λ and λ' would potentially improve the estimation and prediction performance but would also increase the computational cost of model selection.

To investigate this further, we have conducted additional experiments to illustrate the impact of assigning different values to λ and λ' in model NFL. We follow the experimental setup outlined in Section 4.1.1, where the true matrix coefficient exhibits a two-dimensional geometric shape, and the true vector coefficient follows a local constant structure, generated according to scheme (S2). The tuning parameters are set as:

$$\rho = \alpha_1 \|\text{mat}(X^\top y)\|_2, \quad \lambda = \alpha_2 \|Z^\top y\|_\infty, \quad \lambda' = \alpha'_2 \|Z^\top y\|_\infty,$$

where each $\alpha_1, \alpha_2, \alpha'_2$ is selected from a large grid of values in the range of 10^{-3} to 1 with 20 equally divided grid points on the \log_{10} scale.

The running time for model selection, the estimation error, and the prediction error are presented in Table 9, comparing the performance of selecting λ and λ' independently with that of fixing $\lambda = \lambda'$. We can see from Table 9 that both estimation error and prediction accuracy have a clear improvement when λ and λ' are chosen independently. This comes, as expected, at the cost of significantly increased computational time for model selection.

Table 9: Comparison of tuning parameter strategies on model NFL. “Fixed $\lambda = \lambda'$ ” refers to the tuning parameter strategy where we fix $\lambda = \lambda'$, “Indep. $\lambda \& \lambda'$ ” represents the strategy where we select λ and λ' independently, and “Optimal $(\rho, \lambda, \lambda')$ ” denotes the parameters identified as optimal through the model selection process.

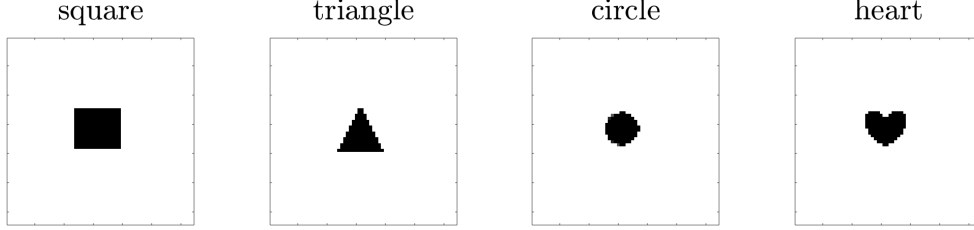
B	Strategy	Optimal $(\rho, \lambda, \lambda')$	RMSE- y	Error- B	Error- γ	Time
Square	Fixed $\lambda = \lambda'$	(57.9, 3.04, 3.04)	9.28	0.11	0.18	0:08:33
	Indep. $\lambda \& \lambda'$	(57.9, 1.02, 9.03)	6.44	0.09	0.10	3:21:40
Triangle	Fixed $\lambda = \lambda'$	(585, 35.1, 35.1)	10.98	0.13	0.23	0:07:38
	Indep. $\lambda \& \lambda'$	(283, 3.96, 50.5)	9.12	0.12	0.16	3:06:40
Circle	Fixed $\lambda = \lambda'$	(244, 11.5, 11.5)	9.82	0.12	0.21	0:08:42
	Indep. $\lambda \& \lambda'$	(118, 1.86, 16.5)	7.71	0.10	0.12	3:28:20
Heart	Fixed $\lambda = \lambda'$	(126, 5.57, 5.57)	10.83	0.13	0.21	0:08:28
	Indep. $\lambda \& \lambda'$	(541, 11.5, 70.9)	8.94	0.12	0.15	3:20:00

In practice, we suggest considering this trade-off based on the specific application requirements. When computational resources are limited, setting $\lambda = \lambda'$ might offer a practical compromise. However, for prediction accuracy is important and computational time is enough, tuning λ and λ' independently can provide better results.

C.3 Two Dimensional Shapes

The true shapes of $B \in \mathbb{R}^{64 \times 64}$ used in Section 4.1.1 are visualized in Figure 4.

Figure 4: The true shapes of $B \in \mathbb{R}^{64 \times 64}$ used in Section 4.1.1



Funding

The research of Meixia Lin was supported by the Ministry of Education, Singapore, under its Academic Research Fund Tier 2 grant call (MOE-T2EP20123-0013) and the Singapore University of Technology and Design under MOE Tier 1 Grant SKI 2021_02_08. The research of Yangjing Zhang was supported by the National Natural Science Foundation of China under grant number 12201617.

References

- [1] G. Bassett Jr and R. Koenker. Asymptotic theory of least absolute error regression. *Journal of the American Statistical Association*, 73(363):618–622, 1978.
- [2] H. Begleiter. EEG Database. UCI Machine Learning Repository, 1999.
- [3] M. Bogdan, E. Van Den Berg, C. Sabatti, W. Su, and E. J. Candès. SLOPE—Adaptive variable selection via convex optimization. *The Annals of Applied Statistics*, 9(3):1103–1140, 2015.
- [4] J.-F. Cai, E. J. Candès, and Z. Shen. A singular value thresholding algorithm for matrix completion. *SIAM Journal on Optimization*, 20(4):1956–1982, 2010.
- [5] C. Chen, Y.-J. Liu, D. F. Sun, and K.-C. Toh. A semismooth Newton-CG based dual PPA for matrix spectral norm approximation problems. *Mathematical Programming*, 155(1):435–470, 2016.
- [6] J. Cui and G. Y. Yi. Variable selection in multivariate regression models with measurement error in covariates. *Journal of Multivariate Analysis*, 202:105299, 2024.
- [7] Y. C. Eldar and M. Mishali. Robust recovery of signals from a structured union of subspaces. *IEEE Transactions on Information Theory*, 55(11):5302–5316, 2009.
- [8] A. Elsener and S. van de Geer. Robust low-rank matrix estimation. *The Annals of Statistics*, 46(6B):3481–3509, 2018.
- [9] J. Fan, W. Gong, and Z. Zhu. Generalized high-dimensional trace regression via nuclear norm regularization. *Journal of Econometrics*, 212(1):177–202, 2019.
- [10] J. Fan, W. Wang, and Z. Zhu. A shrinkage principle for heavy-tailed data: High-dimensional robust low-rank matrix recovery. *The Annals of Statistics*, 49(3):1239–1266, 2021.

- [11] J. Fang and G. Y. Yi. Matrix-variate logistic regression with measurement error. *Biometrika*, 108(1):83–97, 2021.
- [12] J. Fang and G. Y. Yi. Regularized matrix-variate logistic regression with response subject to misclassification. *Journal of Statistical Planning and Inference*, 217:106–121, 2022.
- [13] Y. Feng and S. Wang. A forecast for bicycle rental demand based on random forests and multiple linear regression. In *2017 IEEE/ACIS 16th International Conference on Computer and Information Science (ICIS)*, pages 101–105, 2017.
- [14] J. Friedman, T. Hastie, and R. Tibshirani. A note on the group Lasso and a sparse group Lasso. *arXiv preprint arXiv:1001.0736*, 2010.
- [15] D. Gabay and B. Mercier. A dual algorithm for the solution of nonlinear variational problems via finite element approximation. *Computers & Mathematics with Applications*, 2(1):17–40, 1976.
- [16] C. J. Geyer. On the asymptotics of constrained M-estimation. *The Annals of Statistics*, 22(4):1993–2010, 1994.
- [17] R. Glowinski. *Numerical Methods for Nonlinear Variational Problems*. The Tata Institute of Fundamental Research, Bombay Springer-Verlag, 1980.
- [18] R. Glowinski and A. Marroco. Sur l’approximation, par éléments finis d’ordre un, et la résolution, par pénalisation-dualité d’une classe de problèmes de Dirichlet non linéaires. *Revue française d’automatique, informatique, recherche opérationnelle. Analyse numérique*, 9(R2):41–76, 1975.
- [19] H. Hung and C.-C. Wang. Matrix variate logistic regression model with application to EEG data. *Biostatistics*, 14(1):189–202, 2013.
- [20] L. Jacob, G. Obozinski, and J.-P. Vert. Group Lasso with overlap and graph Lasso. In *Proceedings of the 26th Annual International Conference on Machine Learning*, pages 433–440, 2009.
- [21] K. Jiang, D. F. Sun, and K.-C. Toh. Solving nuclear norm regularized and semidefinite matrix least squares problems with linear equality constraints. *Discrete Geometry and Optimization*, pages 133–162, 2013.
- [22] K. Jiang, D. F. Sun, and K.-C. Toh. A partial proximal point algorithm for nuclear norm regularized matrix least squares problems. *Mathematical Programming Computation*, 6(3):281–325, 2014.
- [23] K. Knight and W. Fu. Asymptotics for Lasso-type estimators. *The Annals of Statistics*, 28(5):1356–1378, 2000.
- [24] M. Kowalski. Sparse regression using mixed norms. *Applied and Computational Harmonic Analysis*, 27(3):303–324, 2009.
- [25] B. Kummer. Newton’s method for non-differentiable functions. *Advances in Mathematical Optimization*, 45:114–125, 1988.
- [26] M. Li and L. Kong. Double fused Lasso penalized LAD for matrix regression. *Applied Mathematics and Computation*, 357:119–138, 2019.
- [27] M. Li, Q. Guo, W. Zhai, and B. Chen. The linearized alternating direction method of multipliers for low-rank and fused Lasso matrix regression model. *Journal of Applied Statistics*, 47(13-15):2623–2640, 2020.

- [28] M. Li, L. Kong, and Z. Su. Double fused Lasso regularized regression with both matrix and vector valued predictors. *Electronic Journal of Statistics*, 15:1909–1950, 2021.
- [29] X. Li, D. F. Sun, and K.-C. Toh. A highly efficient semismooth Newton augmented Lagrangian method for solving Lasso problems. *SIAM Journal on Optimization*, 28(1):433–458, 2018.
- [30] X. Li, D. F. Sun, and K.-C. Toh. On efficiently solving the subproblems of a level-set method for fused Lasso problems. *SIAM Journal on Optimization*, 28(2):1842–1866, 2018.
- [31] X. Li, D. F. Sun, and K.-C. Toh. An asymptotically superlinearly convergent semismooth Newton augmented Lagrangian method for linear programming. *SIAM Journal on Optimization*, 30(3):2410–2440, 2020.
- [32] Y. Li, B. Nan, and J. Zhu. Multivariate sparse group Lasso for the multivariate multiple linear regression with an arbitrary group structure. *Biometrics*, 71(2):354–363, 2015.
- [33] M. Lin, Y.-J. Liu, D. F. Sun, and K.-C. Toh. Efficient sparse semismooth Newton methods for the clustered Lasso problem. *SIAM Journal on Optimization*, 29(3):2026–2052, 2019.
- [34] M. Lin, Y. Yuan, D. F. Sun, and K.-C. Toh. A highly efficient algorithm for solving exclusive Lasso problems. *Optimization Methods and Software*, pages 1–30, 2023.
- [35] Z. Luo, D. F. Sun, K.-C. Toh, and N. Xiu. Solving the OSCAR and SLOPE models using a semismooth Newton-based augmented Lagrangian method. *Journal of Machine Learning Research*, 20(106):1–25, 2019.
- [36] S. Ma, D. Goldfarb, and L. Chen. Fixed point and Bregman iterative methods for matrix rank minimization. *Mathematical Programming*, 128(1-2):321–353, 2011.
- [37] R. Mifflin. Semismooth and semiconvex functions in constrained optimization. *SIAM Journal on Control and Optimization*, 15(6):959–972, 1977.
- [38] J.-J. Moreau. Proximité et dualité dans un espace hilbertien. *Bulletin de la Société Mathématique de France*, 93(2):273–299, 1965.
- [39] G. Obozinski, M. J. Wainwright, and M. I. Jordan. Support union recovery in high-dimensional multivariate regression. *The Annals of Statistics*, 39(1):1–47, 2011.
- [40] J. A. Onton and S. Makeig. High-frequency broadband modulation of electroencephalographic spectra. *Frontiers in Human Neuroscience*, 3:1–18, 2009.
- [41] S. Petry, C. Flexeder, and G. Tutz. Pairwise fused Lasso. Technical Report 102, Department of Statistics, University of Munich, 2011.
- [42] D. Pollard. Asymptotics for least absolute deviation regression estimators. *Econometric Theory*, 7(2):186–199, 1991.
- [43] L. Qi and J. Sun. A nonsmooth version of Newton’s method. *Mathematical Programming*, 58(1):353–367, 1993.
- [44] R. T. Rockafellar. Monotone operators and the proximal point algorithm. *SIAM Journal on Control and Optimization*, 14(5):877–898, 1976.
- [45] R. T. Rockafellar and R. J.-B. Wets. *Variational Analysis*, volume 317. Springer Science & Business Media, 2009.

- [46] Y. She. Sparse regression with exact clustering. *Electronic Journal of Statistics*, 4(none): 1055 – 1096, 2010.
- [47] D. F. Sun and J. Sun. Semismooth matrix-valued functions. *Mathematics of Operations Research*, 27(1):150–169, 2002.
- [48] P. Tang, C. Wang, D. F. Sun, and K.-C. Toh. A sparse semismooth newton based proximal majorization-minimization algorithm for nonconvex square-root-loss regression problems. *Journal of Machine Learning Research*, 21(226):1–38, 2020.
- [49] R. Tibshirani. Regression shrinkage and selection via the Lasso. *Journal of the Royal Statistical Society: Series B (Statistical Methodology)*, 58(1):267–288, 1996.
- [50] R. Tibshirani, M. Saunders, S. Rosset, J. Zhu, and K. Knight. Sparsity and smoothness via the fused Lasso. *Journal of the Royal Statistical Society: Series B (Statistical Methodology)*, 67(1):91–108, 2005.
- [51] K.-C. Toh and S. Yun. An accelerated proximal gradient algorithm for nuclear norm regularized linear least squares problems. *Pacific Journal of Optimization*, 6(15):615–640, 2010.
- [52] O. Wahltinez, A. Cheung, R. Alcantara, D. Cheung, M. Daswani, A. Erlinger, M. Lee, P. Yawalkar, P. Lê, O. P. Navarro, M. P. Brenner, and K. Murphy. COVID-19 Open-Data a global-scale spatially granular meta-dataset for coronavirus disease. *Scientific Data*, 9(1):162, 2022.
- [53] G. A. Watson. Characterization of the subdifferential of some matrix norms. *Linear Algebra and its Applications*, 170(1):33–45, 1992.
- [54] C. Wei. Asymptotics for regularized matrix regressions. *Journal of Mathematics*, 42(2): 146–152, 2022.
- [55] Z. Yang. *A Study on Nonsymmetric Matrix-Valued Functions*. Master’s thesis, Department of Mathematics, National University of Singapore, Singapore, 2009.
- [56] K. Yosida. *Functional Analysis*. Springer, 1964.
- [57] M. Yuan and Y. Lin. Model selection and estimation in regression with grouped variables. *Journal of the Royal Statistical Society: Series B (Statistical Methodology)*, 68(1):49–67, 2006.
- [58] Y. Zhang, N. Zhang, D. F. Sun, and K.-C. Toh. An efficient Hessian based algorithm for solving large-scale sparse group Lasso problems. *Mathematical Programming*, 179:223–263, 2020.
- [59] X.-Y. Zhao, D. F. Sun, and K.-C. Toh. A Newton-CG augmented Lagrangian method for semidefinite programming. *SIAM Journal on Optimization*, 20(4):1737–1765, 2010.
- [60] H. Zhou and L. Li. Regularized matrix regression. *Journal of the Royal Statistical Society: Series B (Statistical Methodology)*, 76(2):463–483, 2014.
- [61] Y. Zhou, R. Jin, and S. C.-H. Hoi. Exclusive Lasso for multi-task feature selection. In *Proceedings of the Thirteenth International Conference on Artificial Intelligence and Statistics*, pages 988–995, 2010.